8-2005

ANALYSES OF HIGH RESOLUTION HYPERSPECTRAL IMAGERY FOR CHARACTERIZATION OF PONDEROSA PINE WOODLANDS

Cullen R. Robbins
University of Nebraska-Lincoln

ANALYSES OF HIGH RESOLUTION HYPERSPECTRAL IMAGERY FOR CHARACTERIZATION OF PONDEROSA PINE WOODLANDS

By

Cullen R. Robbins

A THESIS

Presented to the Faculty of

The Graduate College at the University of Nebraska

In Partial Fulfillment of Requirements

For the Degree of Master of Science

Major: Natural Resource Sciences

Under the Supervision of Professor David A. Wedin

Lincoln, Nebraska

August, 2005

ANALYSES OF HIGH RESOLUTION HYPERSPECTRAL IMAGERY FOR CHARACTERIZATION OF PONDEROSA PINE WOODLANDS

Cullen Robbins, M. S.

University of Nebraska, 2005

Advisor: David A. Wedin

The Bessey Unit of the Nebraska National Forest is a planted ponderosa pine forest located in the Nebraska Sand Hills. Planted in the early 20th Century, it provides a unique opportunity to study the effects of ponderosa pine establishment on the surrounding grassland ecosystem and the effects of increasing pine density on the forest ecosystem. It has been hypothesized that there are key levels of canopy cover at which shifts in ecosystem function occur. The goal of this research was to use remotely sensed data to develop a reliable method for estimating canopy cover. More specifically, canopy cover was estimated by evaluating the relationship between a series of spectral indices applied to data acquired from an AISA overflight of the NNF and measures of vegetation cover (predominantly Leaf Area Index) on the ground. LAI was estimated with a hemispheric camera system and/or a ceptometer in each of eight 40 m x 40 m plots and at each of 97 randomly selected points within the flightline. The hemispheric camera system was shown to be more effective than the ceptometer for measuring LAI in the plots selected for this project. Within these plots, at least three measurements placed approximately 15 meters apart were necessary to capture the range of variability within a plot. The Normalized Difference Vegetation Index (NDVI), Visible Atmospherically Resistant Index (VARI), Wide Dynamic Range Vegetation Index (WDRVI), and Green

Normalized Difference Vegetation Index (GNDVI) all showed a bimodal distribution of pixels and performed well when tested with discriminant function analyses, indicating their potential utility for estimating canopy cover. Of the indices tested, VARI showed the best correlations with LAI at all but the finest spatial resolution and was sensitive to changes in LAI up to the maximum LAI values observed in ponderosa pine.

ACKNOWLEDGEMENTS

I would like to extend my deepest gratitude to my advisor, Dr. David A. Wedin for his expertise and guidance throughout my graduate program. His knowledge, patience, and input have been invaluable during the past 4 years.

I would also like to thank Dr. James W. Merchant and Dr. Geoffrey M. Henebry for serving on my graduate committee. Their input and suggestions were an integral part of this thesis research, and their critical reviews of the thesis were greatly appreciated.

Special thanks goes to the technicians and research assistants who helped gather data at the BU/NNF, often in less than ideal conditions. Technicians Kenneth Elgersma and Waylon Hullinger were extremely capable and helpful for collection of data in the field. Fellow graduate students Xiaoping Deng and Jeff Hellerich also provided assistance collecting data at the BU/NNF, and without their efforts, the thesis would not have been completed. Thanks also to the officemates and fellow graduate students who have provided guidance and diffused tension and stress with their humor and positive attitudes: Kimberly Payne, Kathy Eggemeyer, and Jeremy Hiller.

The Center for Advanced Land Management Information Technologies (CALMIT) provided the platform from which remotely sensed data was acquired. Special thanks to Rick Perk, who was the liaison between myself and the data acquisition team for the AISA sensor system. His patience was greatly appreciated.

I would also like to thank the many friends and family members who have provided moral support and spiritual guidance throughout my graduate program. Their support has been and will continue to be an integral part of any successes that I achieve.

This project was supported by the McIntire-Stennis USDA Forest Research Program and the Sandhills Biocomplexity Project, in grants to Dr. David A. Wedin and the School of Natural Resource Sciences, University of Nebraska-Lincoln.

TABLE OF CONTENTS

Chapter 5

Summary and Future Research

References

Appendix I

Summary of Vegetation Indices

LIST OF TABLES

Chapter 1

Introduction and Research Hypotheses

Chapter 2

Analysis of the Bimodal Distribution of Pixels for Vegetation Indices Derived from AISA Imagery

Chapter 4

Estimating Biophysical Parameters with Remotely Sensed AISA Imagery

LIST OF FIGURES

Chapter 1

Introduction and Research Hypotheses

Chapter 2

Analysis of the Bimodal Distribution of Pixels for Vegetation Indices Derived from AISA Imagery

Chapter 4

Estimating Biophysical Parameters with Remotely Sensed AISA Imagery

Chapter 1

Introduction and Research Hypotheses

Open-wooded ecosystems

Across the world, open wooded ecosystems play an important part in ecological functioning. Defined as a community or landscape with a continuous grass layer and scattered trees, these ecosystems cover approximately 13% of the global land surface, including approximately half the area of Africa, Australia, and North and South America (Scholes and Archer, 1997; Asner, et al., 1998). In North America, savannas and open wooded ecosystems cover over 50 million ha (McPherson, 1997). These systems in North America include Midwestern bur oak savannas, pinyon-juniper vegetation complexes in the southwest and intermontane regions, mesquite grasslands in Texas and the southwest, pine/oak woodlands in the southeastern coastal plane, and ponderosa pine woodlands at lower elevations throughout the Central and Northern Rocky Mountains (Richardson, 1998; Archer, 1990). These ecosystems, each with their own distinct variation in allocation of woody and herbaceous species, play an important role in carbon and nutrient cycles, respiration, and release of trace gases to the atmosphere (Asner, et al., 1998).

Although traditional ecological theory has emphasized grasslands and forests (i.e. relatively closed-canopy wooded ecosystems), an increased awareness of open-canopied savanna and woodland ecosystems is being driven by concerns for conservation, forest health, range management, fire behavior, and carbon sequestration. In particular, changes in the distribution and density of savanna and open woodland ecosystems are a major component of the global story of changing land cover and land use. The ecology of

different savanna ecosystems differs greatly, but they present some common problems for ecological research and monitoring. Trees within savannas are unevenly distributed, patchy, and non-continuous. As a result of these characteristics, the ecosystem becomes a fine-scaled mosaic of open, closed, and intermediate sites. Ecosystem dynamics, including microclimate, plant and animal communities, and soil processes are heavily influenced by that mosaic. Average values for ecological parameters across open and closed locations may not reflect the true values of either type of location.

In the United States, recent attention has been paid to coniferous woodlands because of their susceptibility to fire. Federal legislation, the Healthy Forests Restoration Act (HFRA) of 2003, was signed into law in December of 2003. This act provides funding aimed at condition assessment, restoration and rehabilitation of forests throughout the American West. This adds further impetus for the study of woodlands and their effect on the surrounding environment.

Changes in canopy structure over space and time play a critical role for both ecologists and land managers working with semi-arid wooded ecosystems. Canopy structure is the single most important parameter to measure when observing the response of vegetation to changing environmental conditions and disturbance regimes. At the same time, it is often the best predictor of the effect vegetation structure will have on key ecological and management variables. From an ecological perspective, how do changes in canopy structure affect the availability of resources and the distribution of other plant species when natural constraints (such as fire) are removed? And from a management perspective, have changes in canopy structure negatively affected the ability of forest stewards to prevent catastrophic events? Answers to both questions rely on information

about how the canopy is structured and distributed. The goal of this thesis is to investigate remote sensing and Leaf Area Index (LAI) as a method for describing canopy structure and distribution.

Open-wooded ecosystems in Nebraska

In Nebraska, the presence and expansion of forested areas has not only been the result of reduced fire frequency and increased grazing, but also a result of human interaction. In the late 19th and early 20th centuries, Professor Charles E. Bessey led an effort to introduce ponderosa pine into the Nebraska Sand Hills (Henzlik, 1965). This unprecedented attempt to plant trees in central Nebraska has resulted in a 10,000 ha area set aside as a National Forest preserve: the Bessey Unit of the Nebraska National Forest (BU/NNF) at Halsey, NE (Figure 1.1). The BU/NNF is located in the Sand Hills of central Nebraska (41° 53.38' N, 100° 20.51' W). This forest consists of predominantly ponderosa pine (*Pinus ponderosa),* with some stands of eastern red cedar (*Juniperus virginiana*), and jack pine (*Pinus banksiana).* Within these forested areas, canopy cover can be highly variable as a result of topography, which in turn affects water availability and resource distribution. The grassland areas contain several shortgrass prairie species, including little bluestem (*Schizachyrium scoparium),* shrubs such as leadplant (*Amorpha canescens*), yucca (*Yucca glauca*), and wild rose (*Rosa arkansa*), and some patches of taller shrubs (wild plum (*Prunus domestica)* and sand cherry (*Prunus pumila*)).

The BU/NNF is somewhat anomalous in that the forested area was planted and occurs in an area of stabilized sand dunes in the Nebraska Sand Hills. However, the area does allow for study of ponderosa pine at different density levels where initial (pre-planting) conditions were uniform and management is well-documented. Any findings

not only have potential implications for other ponderosa pine forests, but also for studies involving the effects of this forested area on the Sand Hills ecosystem in which it occurs.

The Nebraska Sand Hills region represents the largest continuous tract of dune sand in the Western Hemisphere (Henzlik, 1965). The topography in the Sand Hills region consists of linear, symmetrical ridge dunes that form diagonally from the NW to the SE. Soil development consists of thin A horizons with very little organic matter, and very little subsoil development. These soils occur on wind-deposited sand. The Sand Hills occur in a semi-arid region where annual mean precipitation at the BU/NNF is approximately 543 mm/yr (1935-1990). 72% of the mean annual precipitation occurs during the May-October growing season. Snow makes up the majority of the winter precipitation which occurs from November to April. Average annual temperature is 9.2° C. The average high and low temperatures in mid-summer (July) are 31.9° and 15.5° C. In winter, the average high and low temperatures during the coldest month (January) are 1.8° and -12.5° respectively. Prevailing winds are from the South in summer and from the North-Northwest in winter.

Historically, management of the forested areas at BU/NNF consisted mainly of cattle grazing. Recently, in an effort to prevent catastrophic fire, the Forest Service has initiated its own forest fire prevention plan, which involved the thinning/cutting of over 4000 acres of land. A significant portion (approximately 1/3) of the forest was disturbed by fire in 1965, while the rest of the forest has remained unburned since planting (trees were planted in the early 1900's and again in the 1930's) (Hunt, 1965). As evidenced by images taken of the area, tree density remains different in the burned and unburned areas of the forest (Figure 1.2). A less dense savanna-type cover predominates in the area

burned by the fire, while closed-canopy forests are common in the unburned section of the forest (Figure 1.2). The less dense, open canopied areas seem more typical of the ecosystem that would prevail under a low intensity, high frequency fire regime, which was more representative of ponderosa pine forests historically (Keeley and Zedler, 1998; Fulé, et al., 1997).

Ponderosa Pine Ecology

Ponderosa pine occurs mainly in relatively open, pure stands at the lower elevations of montane forests (Richardson and Rundel, 1998). Pines hold a competitive advantage over other conifers and deciduous trees in some environments for a few reasons. First, they can thrive on less fertile soils (Richardson and Rundel, 1998). Second, pines tend to have higher water use efficiency and subsequently are more resistant to drought conditions (Rundel and Yoder, 1998; Agee, 1998). Ponderosa pine, in particular, is typically found in environments characterized by cool to cold winters, warm, dry summers and periods of drought-like conditions (Agee, 1998). Historically, ponderosa pines were adapted to frequent, small intensity fires (occurring every 2-20 years) that would help create or maintain an open canopy structure, promote nutrient cycling, regulate species composition, and keep understory biomass at a relative minimum, preventing both tree mortality and sufficient fuel accumulation to produce potentially fatal, high intensity crown fires (Fulé, et al., 1997; Keeley and Zedler, 1998).

Pines are relatively shade intolerant, which in combination with the less fertile, more arid areas in which they occur, may restrict leaf production (Alexander, 1986). Additionally, because of their shade intolerance, there is little advantage for pines to self-shade their leaves, which is obviously important to how leaves are distributed in pines.

As a result, ponderosa pine canopies in semi-arid landscapes tend to be more open with lower Leaf Area Index (LAI) values (Law, et al., 2001). LAI is measured as the half-leaf surface area per unit ground area (m^2/m^2). Ponderosa pines also utilize a self-pruning mechanism that limits the occurrence of dead branches on the tree and possess thick bark that protects the tree from damage (Agee, 1998; Keeley and Zedler, 1998). In even-aged, dense canopies, the self-pruning mechanism seems more prevalent than in less dense, open-wooded areas. Perhaps a response to light, this difference can potentially cause problems for accurate estimation of LAI.

Leaf Area Index in open-wooded ecosystems

Generally, the most widely accepted method for accurate estimation of LAI involves the use of allometric relationships developed from destructive sampling. However, because these relationships are highly site-specific and difficult to develop (they usually require harvesting of several entire trees), they are not feasible in many situations. Fortunately, alternatives exist for LAI estimation, including the use of optical methods, such as an LAI-2000 plant canopy analyzer, or, as is the case with this project, a digital camera utilizing a hemispheric lens. While these methods are useful for quick, nondestructive estimation of LAI, they are not without fault. Optical methods view the canopy from below, so estimates of LAI are in reality a measure of plant area index (PAI), which includes woody, non-photosynthetic materials such as the trunk of the tree. These non-photosynthetic portions of the tree intercept light, but are obviously not leaf area, and therefore confound estimates of LAI. Also, optical measurements of LAI assume random distribution of leaves and shoots, but conifer canopies are highly organized at the needle, shoot, and tree scale. Gower and Norman (1991) found optical

estimates of LAI were 35-40 % lower than LAI determined through site-specific allometric equations in conifer plantations. Law, et al (2001) presented a synopsis of the issues that arise when dealing with optical estimates of LAI as well as methods used to deal with these problems. This study was conducted on the "Oregon Transect", which is a predominantly ponderosa pine forest located in central Oregon. This area has been the subject of several studies involving LAI estimation and remote sensing. In this study, leaf area was estimated using a Licor LAI-2000 plant canopy analyzer along with correction factors that were designed to correct for several sources of error that affect LAI estimation. These correction factors included corrections for clumping of needles within the shoot, at scales larger than the shoot, and woody-to-total area ratio. These correction factors addressed the nonrandom distribution of leaves at the shoot level, the nonrandom distribution of leaves and branches in space, and the effect of woody (non-photosynthetic) vegetation on the estimation of LAI. Law et al (2002) found that allometric equations estimate higher LAI than the LAI-2000 methods. Additionally, the results supported an assumed theoretical maximum LAI of 3 in ponderosa pine forests in central Oregon due to the dry climate. Because the Nebraska Sand Hills are also located in a dry climate, it is assumed that LAI within the BU/NNF will not exceed this theoretical maximum. This assumption will be addressed within the thesis study.

Remote Sensing Overview

Because of its large areal coverage and spectral resolution, remote sensing, or more specifically, spaceborne and airborne imaging sensors, offers a useful tool for investigating forested areas, particularly variation in canopy cover or density. Remote sensing technology has allowed measurements of ecological processes made at local

levels to be extrapolated over large areas. Traditionally, these types of studies make use of vegetation indices, which are designed to respond to differences in plant reflectance characteristics, which are in turn a response to ecological variables. The Normalized Difference Vegetation Index (NDVI), for example, is the most widely used index for assessment and monitoring of biophysical properties such as Leaf Area Index (LAI), vegetation fraction, fraction of photosynthetically absorbed radiation (fPAR), and net primary production. The NDVI relies on the spectral contrast between the strong absorption in the red range (app. 670 nm) of the electromagnetic spectrum and the strong reflectance in the near-infrared range (above 700 nm) of the spectrum that characterizes green vegetation (Gitelson, 2003). While NDVI is not without flaws, it has remained the standard index for vegetation studies because of its well-documented history and easy calculation.

One of the major flaws with the NDVI is that it loses sensitivity in denser canopies. In agricultural studies, where maximum LAI values can reach 6 or higher, the NDVI was insensitive to changes vegetation fraction above 60%, or LAI values above 2 (Gitelson, 2003; Carlson and Ripley, 1997; Gamon, et al., 1995). The LAI in pine canopies typically ranges from 2 to 4 (Richardson and Rundel, 1998), while in ponderosa pine canopies, the theoretical maximum of LAI is around 3 (Law, et al., 2001), still well above the NDVI sensitivity threshold of 2. For this reason, several indices will be tested for their sensitivity to biophysical parameters, including an index that modifies the NDVI for increased sensitivity to higher values of LAI (Table 1.1). A detailed description of the indices chosen can be found in Appendix I.

In this study, the goal is to use remotely sensed data in the form of vegetation indices to determine ponderosa pine canopy structure, which will be measured as LAI. Numerous studies have looked at the relationship between spectral data and LAI in conifer canopies. Spanner et al (1990) studied the relationship between LAI in temperate coniferous forests and Landsat TM spectral data in Oregon, California, and Montana. They used allometric equations to estimate LAI and found values that ranged from 1 to 16. NDVI lost sensitivity to increased LAI at LAI values around 5 to 6, which is higher than had been reported by others, but fairly coincident with a value of 6 to 8 as determined by Peterson et al (1997). Spanner et al (1990) also found that background reflectance (from understory vegetation, soil, or the forest floor) contributed significantly to the reflectance of forested areas, and consequently, the relationship between LAI and spectral data. Nemani et al (1993) looked at how the variability in canopy conditions and understory contributes to errors in reflectance detected by the Landsat TM sensor. This study also uses LAI as a measure of canopy density and tests the sensitivity of a variety of indices to LAI in a western Montana pine forest. They found that a correction using middle infrared (MIR) data can correct for changes in the NDVI signal resulting from understory materials. Fassnacht et al (1997) used Landsat TM data to estimate LAI in mixed forests. LAI was estimated from leaf litterfall measurements, and from hemispheric images taken below the canopy and analyzed with a Delta-T Image Analyzer. All conifer LAI values were below 4.4, and the coefficient of determination between NDVI and conifer LAI was 0.72 ($p=0.002$). They found generally strong linear relationships between NDVI, simple ratio (SR) ($SR = \rho_{NIR}/\rho_R$) and LAI. Gong et al (1995) used a higher spatial and spectral resolution sensor on 6 sites in the "Oregon

transect". They found a linear relationship between LAI and NDVI with a coefficient of determination of 0.65. They also found that the NDVI saturates before LAI reaches a value of 6, though these LAI estimates included sites with deciduous species. In pines, LAI values were almost uniformly below 2.

While the utility of remote sensing has been well documented, its use in open wooded ecosystems presents unique problems. These areas are defined by the co-occurrence of both woodland and grassland species. In fact, localized areas within these cover types may act as closed canopied forests or open grasslands. Also, the grassland and woodland vegetation types almost certainly influence each other. These patchy vegetation types can change from forest to grassland within a matter of meters on the ground, and therefore, the remote sensing instrument must be capable of assessing this change. Recent studies by University of Nebraska – Lincoln researchers involving grassland/savannah forest interaction at the BU/NNF indicate the existence of a pine density threshold, above which dominant C_4 grasses are excluded, understory grass biomass decreases, and a dense pine needle forest floor develops (unpublished Wedin, et al.). Remote sensing provides a tool to investigate this threshold and other ecological and management issues related to canopy structure over a large area.

The Advanced Very High Resolution Radiometer (AVHRR), Landsat TM, and Moderate Resolution Imaging Spectrometer (MODIS) have been the focus of much research involving the use of remote sensing to retrieve biophysical information because of their widespread use, large areal coverage, and well-documented characteristics. The AVHRR sensor, developed by the National Oceanic and Atmospheric Administration (NOAA), has been widely used as a tool for studying vegetation phenology over large

areas and has been an important instrument in the development of the NDVI. The spatial resolution of the instrument at nadir, however, is 1.1 km, certainly too broad to assess the differences in vegetation that occur in semi arid woodlands at much finer scales. The newer MODIS sensor also has a fairly coarse spatial resolution (250 – 1000 m), though it provides an improved spectral resolution (from 4-6 bands on AVHRR to 36 bands on the MODIS platform). Likewise, the Landsat series of satellites has been widely used for vegetation studies and was also important for the development of NDVI, but the available spatial resolutions (15 m, 28.5 m, and 60m) may be insufficient for detecting subtle changes in the landscape, such as canopy closure, new pine establishment, and woodland expansion where much ecological interest lies (Wu and Strahler, 1994).

Asner et al (1998) has used high spatial resolution hyperspectral remotely sensed data to study savannas in Texas. The imaging spectrometer used in this study is an Advanced Very High Resolution Imaging Spectrometer (AVIRIS), which collects data from 400-2500 nm. This study showed promise for estimating LAI and other vegetation function parameters such as non-photosynthetic vegetation area index (NPVAI) and fraction of photosynthetically active radiation (fPAR) by using inverse modeling, which estimates the structural attributes producing canopy reflectance observed by a remote sensing instrument through mechanistic modeling of the reflectance of a plant canopy.

While research conducted at the BU/NNF has been, until recently, minimal, relevant studies at other Sand Hills locations have been conducted. Wylie et al (1996) tried to test relationships between spectral vegetation indices and biophysical parameters such as LAI, biomass, and pigment concentration across varying levels of herbaceous

standing dead, grassland communities, soil exposures, and soil types at the Niobrara Valley Preserve in north central Nebraska. Data was collected over a single week in early June, so temporal variation in biophysical parameters and their consequent relationship with spectral data is lacking. However, while this research was conducted in grasslands, the findings show that NDVI is sensitive to changes in LAI below a value of 2, which may have implications for findings at the BU/NNF.

Emly et al (1997) used satellite and airborne-derived remote sensing data to identify ecological habitat types and seral stages over the Samuel R. McKelvie National Forest, which is another unit of the Nebraska National Forest. Landsat TM and Xybion multispectral imagery were both used to acquire the remote sensing data. While the data acquisition included the forested area of the McKelvie National Forest, the study focuses on determining broad cover types in grassland areas through the use of discriminate (or discriminant) analysis, where linear combinations of predictor variables (Landsat bands in this case) are used to classify data into known groups (in this case, habitat types or seral groups). While this study focuses on classifying cover into fairly broad groups, it provides an introduction to discriminant function analysis, which was used in part of this thesis research.

At the Niobrara Valley Preserve, Wylie et al (2000) used high resolution (3m) hyperspectral AVIRIS data to map eastern red cedar and ponderosa pine occurrence. The goal of this project was to produce a landcover map where eastern red cedar and ponderosa pine signals were separated and classified. To achieve this objective, a decision tree analysis was used. A decision tree analysis hierarchically subdivides data into subsets of greater uniformity based on thresholds in the input spectral data so that

subset land cover uniformity for each hierarchical level is maximized. Wylie et al (2000) found this method to be effective for mapping these cover types as determined through preliminary accuracy assessments and land cover confidence maps. While the goal of this project was not to use remote sensing to estimate biophysical parameters, it provides some useful information regarding the utility of hyperspectral remotely sensed imagery.

Overview of current project

Because of its high spatial and spectral resolution relative to that of the most commonly used satellite-borne sensors (such as Landsat Thematic mapper (TM), MODIS, and AVHRR data), an AISA sensor was selected to acquire an image over the BU/NNF. The sensor is maintained and owned by the Center for Advanced Land Management Information Technology (CALMIT) at the University of Nebraska – Lincoln (UNL). The AISA sensor is a pushbroom imaging spectrometer, built by Specim Ltd., mounted in a Piper Saratoga aircraft that has been modified to house the sensor. The sensor gathers data at selectable wavelengths between 430 and 900 nm at a selectable spatial resolution. Data can be acquired in any of three modes: full spatial resolution with reduced spectral channels, full spectral resolution, or full spectral with partial spatial resolution. Data for this project was acquired in the full spatial/reduced spectral mode, where 35 – 3nm wide bands between 430 and 900 nm were selected (Table 1.2). In this mode, the spatial resolution was approximately 3m. While this instrument is considered hyperspectral, the inversion of a canopy radiative transfer model as described in Asner et al (1998) cannot be fully duplicated with the AISA data because the AISA data lacks

both the spectral range of the AVIRIS instrument and the continuity through the spectral range, where absorption features in narrow spectral regions can be studied.

The AISA data acquisition over the BU/NNF used in this study occurred on August 10, 2002, starting at approximately 11:28 Central Daylight Time. Three passes over the target area were necessary to cover the desired area. The resulting flightline covered a swath of the forest approximately 11 km long and 900 m wide, covering 990 ha (Figure 1.1). The area contains a wide range of canopy covers, from open grassland to savanna to closed canopy forest. This area also includes six plots previously used by School of Natural Resources (SNR) research projects and two additional plots added for this study. They are part of a larger study that includes approximately 20 plots located throughout the forest. These plots were selected based on canopy cover in an attempt to capture the heterogeneity in canopy cover throughout the entire forest. The eight plots within the flighline include two plots containing only one tree, two plots that were considered open woodlands, one medium density plots, and three high density plots. These plots measure 40m x 40 m, and are divided into 16 - 10 m x 10 m subplots (Figure 1.3). Within each of these plots and subplots, basal area and DBH have been measured. In half of the subplots (1, 3, 6, 8, 9, 11, 14, and 16), measurements were taken with a digital camera fitted with a fisheye lens that acquires an image looking upward from under the canopy for estimation of LAI. Estimated LAI with this system is determined based on the likelihood that light is extinguished at a given angle (light is more likely to be blocked at lower angles near the horizon and less likely directly overhead). The corners of these plots have been geolocated using a GPS unit with differential correction produced by Trimble.

Because there were relatively few large (40 m x 40 m) plots within the flightline, 100 points were randomly chosen throughout the flightline in an effort to more fully capture the range of variability from open, treeless prairie to closed canopy forest. These points were selected from the AISA image that was flown over the area. Each of these points was then visited, where several measurements were taken. At each point, photos were taken with the LAI camera, notes were taken about the surrounding vegetation, and percent cover estimates were recorded to describe ground cover. The percent cover measurements consisted of estimating ground cover according to the following cover types: grass, sand, forest floor, bare sand, and forbs. Measurements were taken so that the cover at each point summed to 100%. The area over which these measurements were taken at each plot was approximately 3m x 3m, which corresponds to the pixel size of the AISA imagery.

Previous research on stand structure at the BU/NNF

Researchers from the School of Natural Resources (UNL) have collected considerable data on the structure and dynamics of ponderosa pine woodlands at BU/NNF since 1999. Because this thesis adds remote sensing analyses to the larger BU/NNF study, it is appropriate to summarize some of the pre-existing data relevant to canopy structure. Although canopy biomass and LAI have not been measured destructively in these plots, reasonable estimates are possible using existing data. These estimates from the relatively dense, closed-canopy pine plots are most reliable because of their homogeneity. One can assume that on a per-unit-area basis (e.g. in 10 m x 10 m subplots), stand measures such as tree density, basal area, leaf biomass, and LAI are relatively uniform throughout dense pine areas. One can also assume that stand structure

is relatively uniform throughout the field of view for the hemispheric lens used in this thesis. This minimizes many of the spatial scaling issues that arise when comparing field data from the plots with either above- or below-canopy non-destructive imagery. If non-destructive methods of canopy analysis cannot reasonably "capture" the even canopy structure of the dense plots, they are unlikely to perform well in the heterogeneous open savanna and woodland plots.

Data on three dense 40 m x 40 m plots (4, 9, and 10) from the original set of 20 were averaged to characterize stand structure for typical closed-canopy pine forests at BU/NNF. Most of the data and methods are found in (Ding, 2002), but some is unpublished (Wedin 2003, 2004). Basal area for these stands averaged 36 m^2/ha, with a mean density of 630 trees / ha. This falls in the basal area range of 30-50 m^2/ha reported for Rocky Mountain ponderosa pine forests by Peet (1988). Covington et al. (1994) argue that most western ponderosa pine stands had lower basal areas and densities prior to fire-exclusion, which began in the late 1800's. They report presettlement basal area of 17 m^2/ha and density of 50 trees / ha for a research area that had a basal area of 42 m^2/ha and a density of 2165 trees /ha in 1987. The high modern stand density (Covington et al. 1994) reflects an uneven size structure with a few large old pines and numerous small diameter pine saplings in the understory, a situation common throughout the west. In contrast, the planted forests at BU/NNF have a relatively even age and size structure (mean age for large trees = 61 yrs, mean dbh = 26cm).

The dense pine stands at BU/NNF have minimal understory vegetation (sparse grasses and shrubs, < 20 g/m^2), but a relatively thick (5 to 15cm) forest floor of fresh and partially decomposed pine needles, cones and branches. The mass of the forest floor is

almost ten times that of typical grassland vegetation in Sand Hills prairie. Annual litterfall was measured in each plot by collecting materials that fell into four dish pans staked to the ground. Samples were collected in November of 2001 and 2003 (no data in 2002). Annual pine needle litterfall (not counting sticks and other detritus) over the two years averaged 340 g m^{-2} yr^{-1}. If one assumes that total canopy biomass is relatively constant from year to year, litterfall is also an estimate of annual needle production. Given the mass of the forest floor and annual litterfall, the estimated mean residence time of the forest floor is 6.2 yrs. This is similar to an independent estimate of the time it takes ponderosa pine needles to decompose on the forest floor (6.8yrs) based on a pine needle litterbag decomposition study at BU/NNF (Wedin, unpublished data). Thus, the mean annual litterfall estimate appears to be reasonable.

Given mean annual litterfall, one can estimate total canopy (i.e., live needle) biomass if they know needle longevity. Elgersma and Wedin (unpublished) measured the biomass of needle cohorts (e.g., 1 year old, 2 year old, etc) for branches collected in all the plots though one calendar year. Total needle biomass was relatively constant across the year. The retention of new needles was high through year three, when most needles were shed. Needle longevity averaged 2.65 yr and did not differ significantly between open-grown and dense pines. Assuming annual needle production of 340 g m^{-2} yr^{-1} and needle longevity of 2.65 yr, total canopy biomass (needles only) for the dense pine stands is estimated at 902 g/m^2.

An independent estimate of canopy biomass is possible using published allometric relationships for ponderosa pine (Gower et al. 1993, Little and Shainsky 1995; see Ding, 2002 for details). When these allometric equations were used to estimate canopy, bole,

bark and branch biomass using the diameter at breast height (DBH) of each tree in the plots, the average aboveground biomass of the dense stands was estimated as 13,000 g/m^2, and average canopy biomass (needles only) is estimated as 898 g/m^2. The two independent estimates of canopy biomass for the dense pine stands are remarkably similar. This appears to be a reasonable estimate of actual canopy biomass for dense pine stands at BU/NNF even though it has not been measured with destructive, whole-tree sample methods. Average aboveground net primary production for the stands is estimated as 430 $g\ m^{-2}\ yr^{-1}$ (80% needle; 20% wood increment, cones, etc).

Specific Leaf Area (SLA), the ratio of leaf area to leaf mass, is needed to estimate canopy leaf area on a tree or area (e.g., LAI) basis. Marshall and Monserud (2003) reported a range of 25 – 45 cm^2/g for ponderosa pine SLA on samples collected throughout the canopy of pine stands in Idaho. Wedin (unpublished) found 27.3 as the SLA of pine needles from five year old ponderosa pine saplings. Given a canopy biomass of 900 g/m^2, canopy LAI probably lies between 2.25 (SLA = 25 cm^2/g) and 2.7 (SLA = 30 cm^2/g) depending on the value of SLA used. This estimate is for total canopy LAI and does not include branches, cones and other non-leaf biomass. Thus, it is likely to differ from non-destructive estimates of LAI presented in this thesis, which are also influenced by non-photosynthetic tissues.

Thesis Overview

The overall objective of this thesis is to assess the utility of remotely sensed data for describing ponderosa pine canopy structure. To achieve this objective, three related studies were designed:

1) The first study involves analyses of vegetation indices derived from hyperspectral imagery to determine which index (or indices) most effectively separates tree from non-tree cover types (Chapter 2). This was done by taking advantage of the pixel distribution that results from the application of each index to the spectral data. Of particular interest is whether the indices derived from hyperspectral imagery are more effective than black and white aerial photographs for discriminating between tree and non-tree cover types?
2) The second study investigates a system used to determine Leaf Area Index (LAI), the measure of canopy cover used in this thesis (Chapter 3). The first goal of this study was to determine how well this indirect measure of canopy cover corresponds to direct measures of stand structure, such as basal area. The second goal of this study was to determine how effectively the hemispheric LAI estimating camera system can describe LAI within a given area, particularly at scales ranging from subplot (3 m x 3 m) to plot (40 m x 40 m).
3) The third study involves comparison of LAI values with index values derived from the hyperspectral imagery (Chapter 4). The goal of this study was to determine how well LAI and various vegetation indices are correlated, and at what resolution the AISA data is most effective for comparison with LAI estimates from the camera system.

Figure 1.1 The National Land Cover Dataset (NLCD) image of Nebraska derived from Landsat ETM+ data with the outline of the Bessey Unit of the Nebraska National Forest shown in red. The forested area of the BU/NNF land is shown in green in the lower image. The blue outline in the lower image highlights the extent of the AISA overflight.

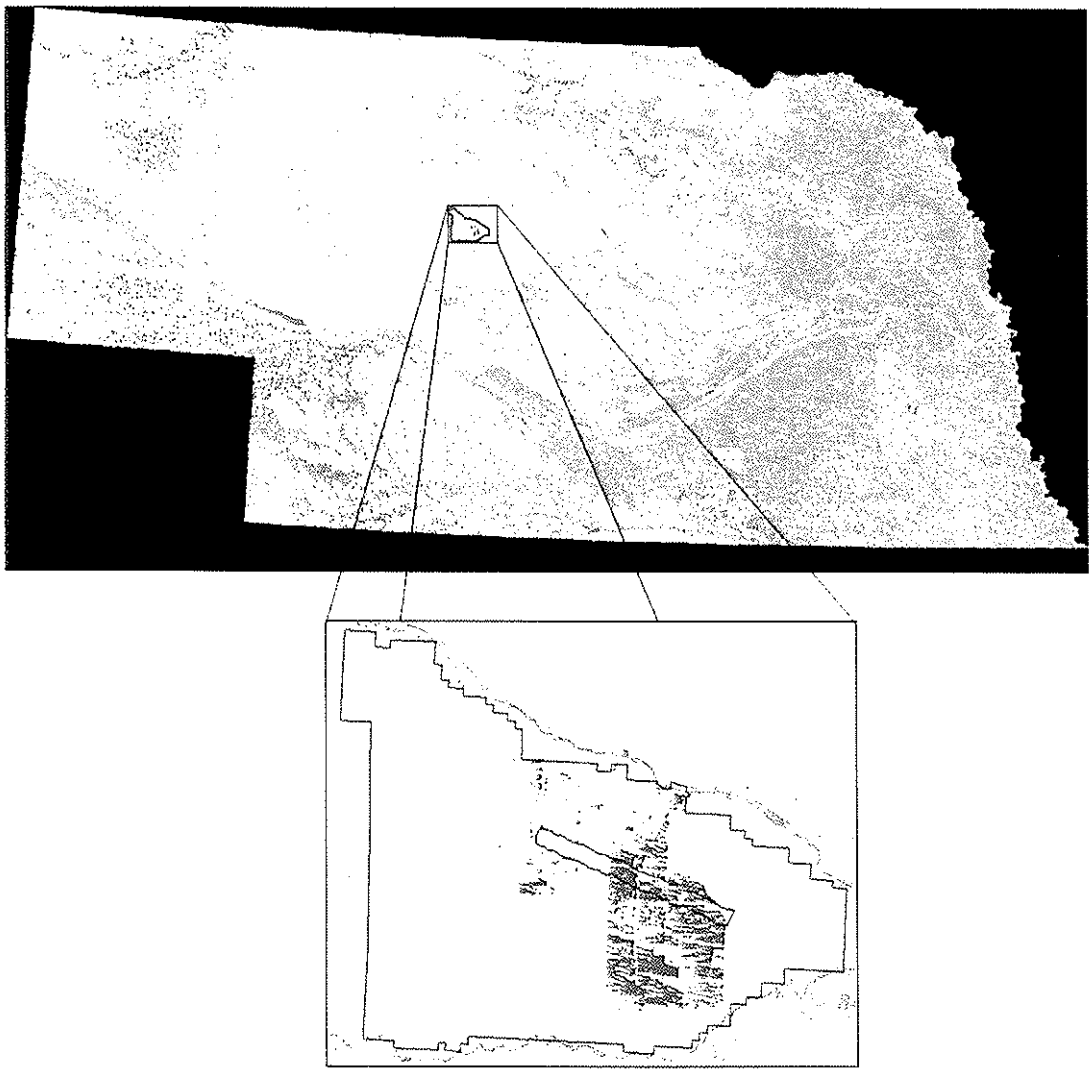

Figure 1.2 Digital Orthophoto of the Nebraska National Forest. The approximate area burned in 1965 is shown between the white lines. Trees appear as the darkest items in the image. The burned area exhibits much lower tree density when compared to the unburned area to the south.

Figure 1.3 The typical layout of the subplots within each plot are shown. Plots were numbered from 1 to 16. Camera LAI measurements were only taken in the plots numbered below. Diameter at Breast Height (DBH) and pine litter biomass were measured in all 16 plots.

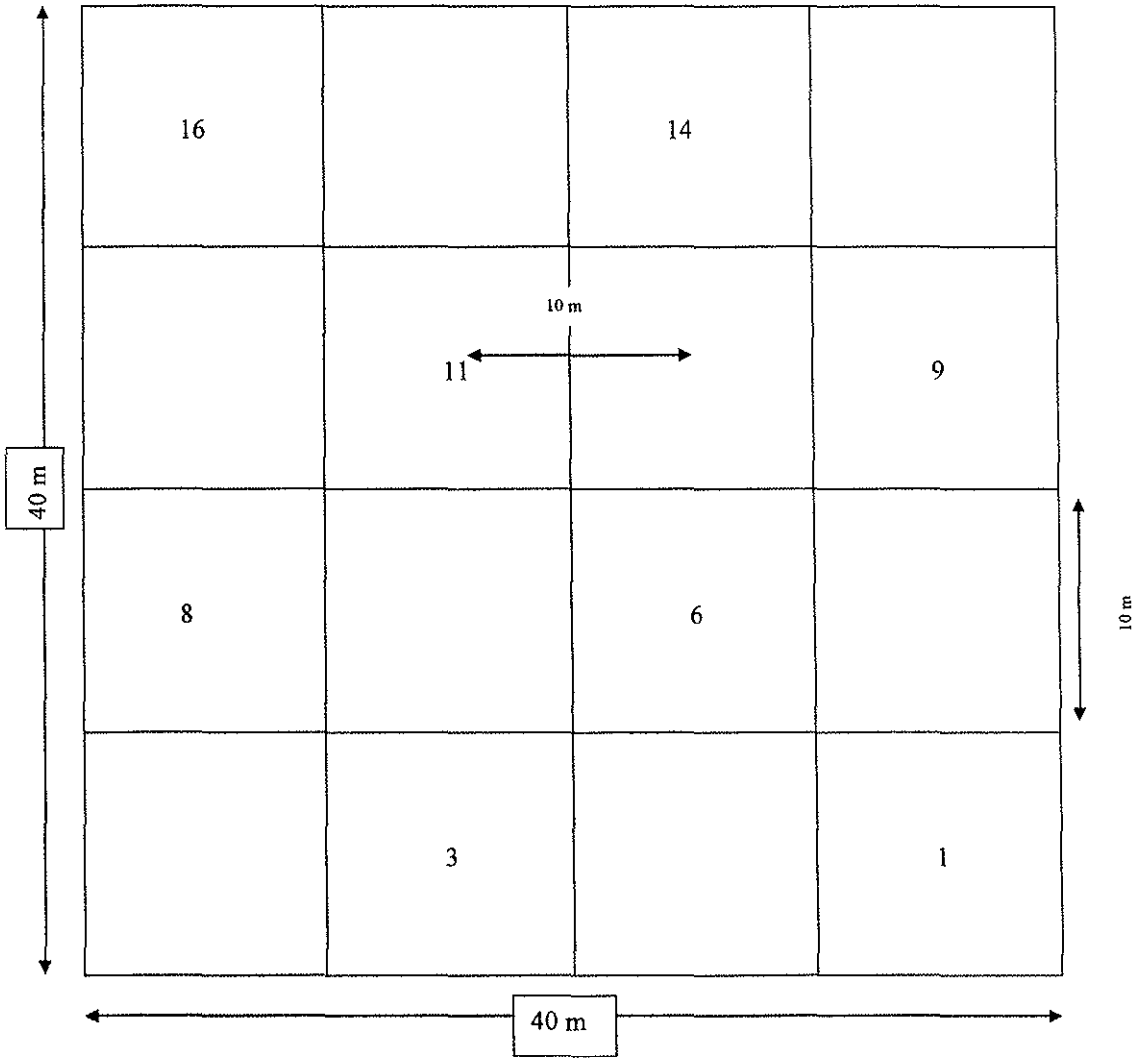

Table 1.1 A summary of proposed vegetation indices

Index	Purpose/Benefit	Citation
1. NDVI – (ρNIR-ρR/ρNIR+ρR) (center of 660-680 for red and shortest in 750-1100 nm area)	Enhance contrast between soil and vegetation but minimize effects of illumination	Rouse, et al., 1974 Galvao, et al., 2000
2. Soil Adjusted Vegetation Index (SAVI) – (ρNIR-ρR)/(ρNIR+ρR+L)(1+L) and/or 1.5((ρNIR-ρR)/(ρNIR+ρR+.5) - L is function of canopy density	Minimizes soil-brightness influences	Baret and Guyot, 1991
3. Wide Dynamic Range Vegetation Index (WDRVI) – (α * ρNIR – ρR)/(α * ρNIR + ρR)	Increases dynamic range of NDVI (increases sensitivity at higher LAIs)	Gitelson, 2003
4. Reciprocal Reflectance Difference Vegetation Index (RRDI) $(1/\rho_{RE} - 1/\rho_{NIR})^* \rho_{NIR}$ or $(1/\rho_G - 1/\rho_{NIR})^* \rho_{NIR}$	Correlated to chlorophyll content in leaves	Gitelson, et al., 2003
5. Green NDVI – $(\rho_{NIR}-\rho_G)/(\rho_{NIR}+\rho_G)$	Maximizes sensitivity to chlorophyll concentration	Gitelson, et al., 1996; Gitelson, et al, 2002; Gitelson, et al, 2001
6. EVI – $G(\rho_{NIR}-\rho_R)/(\rho_{NIR}+C_1\rho_R-C_2\rho_B+L)$ G=2.5, L=1, C_1=6, C_2=7.5	Canopy Background adjustment that accounts for differences in light extinction through the canopy in R and NIR	Huete, et al., 1997
7. VARI – Visible Atmospherically Resistant Index $(\rho_G-\rho_R)/(\rho_G+\rho_R-\rho_B)$ and $(\rho_{700}-1.7\rho_R+0.7\rho_B)/(\rho_{700}+2.3\rho_R-1.3\rho_B)$		Gitelson, et al., 2002

Table 1.2 A summary of the bands selected for the AISA imagery acquisition. The bandwidths are centered on the wavelength given. The third column represents the approximate bandwidths of the Landsat TM sensor as they relate to the AISA bands.

	Wavelength (nm)	Bandwidth (nm)	Corresponding Landsat Band
1	479	3	1
2	496	3	1
3	506	3	1
4	516	3	1
5	524	3	2
6	537	3	2
7	545	3	2
8	555	3	2
9	566	3	2
10	576	3	2
11	584	3	2
12	595	3	2
13	603	3	
14	610	3	
15	627	3	
16	636	3	3
17	643	3	3
18	662	3	3
19	670	3	3
20	681	3	3
21	693	3	
22	700	3	
23	711	3	
24	722	3	
25	740	3	
26	757	3	
27	771	3	4
28	782	3	4
29	799	3	4
30	813	3	4
31	822	3	4
32	845	3	4
33	866	3	4
34	884	3	4
35	895	3	4

Chapter 2

Analysis of the Bimodal Distribution of Pixels for Vegetation Indices Derived from AISA Imagery

Introduction

Semi-arid landscapes are often dominated by shrubland, savanna or woodland cover types, where land cover is a complex mosaic of woody and non-woody vegetation. A broad range of ecological and natural resource management applications require a quantitative description of both the amount and spatial configuration of woody vegetation in such landscapes. These applications may include characterizing habitat for plant or animal species (Thill and Koerth, 2005; Homyak, et al., 2005; Matrai, et al., 2004; Ransome, et al., 2004), parameterizing ecosystem models that predict landscape-scale functioning (Gower and Norman, 1991; Nemani, et al., 1993; Spanner, et al., 1990; Bonan, 1995 and 1993; Running, 1990; Running and Gower, 1991; Gower, et al., 1999), or describing tree canopy cover for forestry or wildfire management (Mitchell and Popovich, 1997; Koutsias and Kateris, 2003). A simple classification of the landscape into two cover types (tree and non-tree) is a starting point in such applications. In some situations, this simple approach alone is a powerful tool. When viewing an aerial photograph, a Digital Orthophoto Quarter Quadrangle (DOQQ), or a Landsat TM image of a semi-arid wooded landscape such as the Bessey Unit of the Nebraska National Forest (BU/NNF), one can easily distinguish trees (in this case, pines and junipers) from other cover types (grassland species, low shrubs, bare soil). For small areas or limited numbers of points, visual inspection of aerial photographs and/or DOQQs can provide a high resolution classification of wooded and non-wooded areas. Such analyses can be time

consuming and are often dependent on a priori knowledge of the cover types within a given area. Therefore, for larger areas, a more sophisticated approach is necessary.

Multi-or hyperspectral sensors have capabilities that cannot be matched by aerial photographs or DOQQs. These sensors offer quantitative data separated by band (or by a combination of consecutive bands) often in wavelengths beyond the range of visible light, and at spatial scales and extents that rival those available for DOQQs and aerial photos. Having quantitative spectral data allows for the study of plant biophysics as they relate to light absorption and/or reflectance by the object or area of interest. The ability to display this information graphically also allows for this biophysical data to be combined with other data types (in a GIS, for example) to study the effects of other influences on the object of interest.

Given the obvious visual difference between tree and non-tree cover types in semi-arid landscapes, it follows that there should be strong differences spectrally. This chapter examines the ability of a series of indices derived from remotely sensed spectral data to distinguish tree and non-tree pixels in an AISA image acquired over the BU/NNF in August of 2002. Given this objective, the ideal spectral index should result in a bi-modal distribution of pixel values. As suggested by visual inspection of aerial photographs, most pixels at this spatial scale either have some tree canopy coverage or they do not. If the objective was to quantify differences in the understory given a particular degree of tree canopy coverage or to quantify the amount (e.g. LAI) or type (e.g. pine vs. juniper) of tree canopy coverage, another spectral index might be more appropriate. Those are not the objectives, however, of this chapter.

Methods

The BU/NNF, located in the Sand Hills of central Nebraska, is a 25,000 ha unit, of which app. 10,000 ha contain trees. The forested areas contain predominantly ponderosa pine (*Pinus ponderosa)* and eastern red cedar (*Juniperus virginiana)*, which were planted in the early 1900s. Within these forested areas, canopy cover can be highly variable as a result of the topography of the area, which in turn affects water availability and resource distribution. The grassland areas contain several shortgrass prairie species, including little bluestem (*Schizachyrium scoparium)*, shrubs such as leadplant (*Amorpha canescens*), yucca (*Yucca glauca*), and wild rose (*Rosa arkansa*), and some patches of taller shrubs (wild plum (*prunus domestica)* and sand cherry (*prunus pumila*)). Note that the term "grassland," in the context of this paper, includes these plant species as well as patches of open sand, which occur intermittently throughout the grassland areas within the Sand Hills.

The AISA image acquisition took place on August 10, 2002, and covered approximately 990 ha of the BU/NNF. The acquisition attempted to cover an area that included a wide range of cover types, including open grassland, savanna-type areas of intermittent tree cover, and densely forested areas. The forested areas within the flightline included some stands of pure cedar, though most of the forested areas were composed of ponderosa pine. For more details on the study area and image acquisition, see Chapter 1.

For this study, seven indices were selected for the analysis of the AISA hyperspectral data. A summary of the indices is provided in Table 1.1 and a more detailed description of the indices is found in Appendix I. Indices that are commonly

used for Landsat TM imagery analysis (NDVI, GNDVI, VARI, and WDRVI) were calculated two different ways, one with specific wavebands chosen from the available AISA wavebands, and one that averaged across several AISA wavebands in an attempt to emulate the Landsat TM bandwidths. A summary of these simulated Landsat wavebands and the AISA wavebands are shown in Table 1.2. Each index was calculated on each pixel of the AISA image data acquired over the BU/NNF. This produced individual images for each index that showed the index values for each pixel in the flightline (Figure 2.1). The histogram describing the distribution of values over the entire flightline for each index was viewed to determine whether a bimodal distribution was present. If such a distribution existed, the value with the lowest number of pixels present between the two modes of the distribution was used as the tree/grass threshold value. This value operationally separates tree from grass in the AISA flightline with the given indices. The distribution for each index along with the threshold value is shown in Figure 2.1.

In addition to the indices, three additional images were used. First, a Digital Orthophoto Quadrangle of the flightline was also classified into tree/non-tree classes based on its bimodal distribution. Second, a principal component analysis was performed on the initial AISA image that contained the full complement of spectral data (35 bands). A principal component analysis reduces the dimensionality of a dataset. This is accomplished by calculating a set of variables that define a projection in n-dimensional space that captures the maximum amount of variance. This projection is the first principal component. Each successive principal component is orthogonal (and therefore unrelated) to the previous principal component in the dataset. Principal components are calculated up to the original number of variables (in this case 35), when all of the

variability in a given dataset has been accounted for. For this analysis, 10 principal components were saved, and the distribution of each principal component was viewed to determine whether a bimodal distribution existed. The first two principal components each showed a bimodal distribution, so they were added to the bimodal analysis and classified as tree/non-tree using the same threshold technique used for the vegetation index images. The distributions and threshold values for these two images are shown in Figure 2.2.

For those images with a bimodal distribution, the data was classified into tree or non-tree categories by applying the threshold value to each index dataset. The resulting classified image is essentially a visual representation of the bimodal distribution, where each mode is classified as either tree or grass. With these images, qualitative differences between images could be visually distinguished. This visual analysis provides a first-order determination of which indices perform the best for separating tree from non-tree.

To quantitatively analyze the bimodal distribution for each of the indices, a discriminant function analysis was used to test how well each of the indices can separate the tree and non-tree cover types. A discriminant function develops rules for assigning unclassified objects into previously defined groups based on some variable of interest. In this case, a discriminant function analysis will test how well index data correctly separates data points into tree and non-tree categories.

Within the flight line of the AISA overflight, approximately 100 points were selected to test using the discriminant function analysis. Each of these points was viewed to determine whether the point was located in either tree or non-tree cover types. Of the 100 points, 34 were located in non-tree areas, 50 were located in tree areas, and 16 were

located in areas where cover type could not be determined visually. These 16 points were excluded from further analysis. Of the remaining 84 points, 11 tree points and 10 non-tree points were randomly selected and withheld from the initial analysis for use as a validation dataset. The remaining 63 points were used as a training dataset. For each index, the discriminant function analysis used the 63 points to produce a function that separated tree from non-tree. Each function was then applied to the training dataset where each point in the training dataset was classified as tree or non-tree according to the function. Then the predicted classes for each of these training points were compared to the actual classes for each point, and the accuracy of the discriminate function was assessed.

Results and Discussion

Indices that are based on or developed from the NDVI, such as the Wide Dynamic Range Vegetation Index (WDRVI), green NDVI, and VARI (including the Landsat emulation indices) all show a distinct bimodal distribution, while the Reciprocal Reflectance Difference Vegetation Indices (using red edge and green wavebands) show more of a unimodal, skewed distribution (Figure 2.1). The Enhanced Vegetation Index (EVI) and the Soil Adjusted Vegetation Index (SAVI) show a normal distribution, indicating the indices discriminate between trees and grassland poorly. The images produced by applying the EVI and SAVI indices support this finding; trees are difficult to distinguish from other cover types. Therefore, these indices will not be used for further analysis.

Of the ten principal components saved from the principal component analysis, only two showed a bimodal distribution (principal components 1 and 2). The third

principal component had a trimodal distribution, but when the image was viewed, the principal component was predominantly noise from the instrument, and therefore was not used.

When compared qualitatively to each other, the indices with a distinct bimodal distribution (NDVI, green NDVI, VARI, and WDRVI) show some subtle differences. The VARI image does a better job of capturing the area of cedar in the central section than the other three indices and also shows less misclassification of grassland areas, where grassland is misclassified as tree (Figure 2.4). The NDVI, VARI, and WDRVI (both Landsat-emulated and regular) differed little from each other, and these differences are difficult to distinguish visually.

While these analyses provide a good first order look at how spectral data from the AISA sensor can be used to discriminate tree from non-tree, there are some imperfections that should be pointed out. First, areas within the grassland are incorrectly classified as trees in the NDVI image (Figure 2.3) while solitary trees are sometimes misclassified as non-tree. The tree misclassifications appear to be a result of plant assemblages within the grassland that are more productive than the surrounding grassland. These plant assemblages may be due to wet areas that allow for higher production, or they may indicate the occurrence of shrubs or other more productive cover types that produce a higher NDVI signal than the rest of the grassland area. The misclassification of individual trees is likely due to the spatial resolution of the image, where a single tree is not large enough to affect the NDVI value of a pixel enough to raise it above the stated threshold.

The first principal component image was the most effective at separating tree from non-tree of all the images (Figure 2.2). In grassland areas, it did not misclassify grassland areas as trees, as was the case with the index-based images. It was also effective at properly classifying the trees in the densely forested areas, while not misclassifying background and shadow as trees. The only errors observed when viewing the image was slight underclassification of individual trees, which is most likely a result of the spatial resolution of the sensor, where small trees did not have a large enough effect on the signal of the pixel to change how the pixel was classified. The second principal component was much less effective than the first principal component at separating tree from non-tree (Figure 2.2). The densely forested areas showed some slight misclassifications where background and/or shadow were misclassified as tree. Grassland areas were also misclassified in some areas, where grassland areas were classified as trees. When compared to the NDVI bimodal image, the second principal component image shows similar trends, where there is some misclassification of both forested and grassland areas.

While the PCA image does the best job of separating tree and non-tree cover types visually, its utility is somewhat limited as an analysis tool because it is not a standardized index with explicit and repeatable calculations. While the results give some indication of the potential power of the hyperspectral data, often the data requires significant manipulation to reach the desired goals. For example, the separation of pine and cedar cover types would be a valuable application. However, this usually requires a separate discriminate function analysis, which teases apart very small differences in the reflectance characteristics of the two cover types.

The results from the index and PCA bimodal classifications were compared to a subset of a DOQQ taken in 1999. The area subset from the DOQQ reflects the exact area of the AISA flightline. The effective resolution of the DOQQ subset is 1 m, compared with the 3m resolution of the AISA imagery. Unlike the AISA imagery, the DOQQ subset is a grayscale image, meaning the image contains only one band of information that is developed by assigning a value between 0 and 255 for each pixel based on its relative brightness. A grayscale image appears "black and white," so that the darkest pixels appear black (value of 0) and the lightest values appear white (value of 255). The histogram of these values for the image shows a bimodal distribution, giving an indication that some separation of tree and grassland may be possible (Figure 2.4). When the threshold between the two modes is applied to the image, the resulting image showed some interesting trends, especially when compared with the images from the AISA indices (Figure 2.4). First, in areas where tree cover was thick, the DOQQ classified image showed a discontinuous tree canopy when compared to the NDVI classified image, possibly a result of the increased spatial resolution. In grassland areas the DOQQ classified image misclassified many areas of grassland as trees. These misclassifications seem to correspond to areas of steep topography, which appear dark in the original DOQQ's. While these areas of steep topography may have plant associations that make them appear darker in the DOQQ, the AISA index images did not have the same problem misclassifying these as trees. These associations suggest these areas appear darker in the DOQ as a result of sun angle differences, i.e. they are north-facing slopes that are generally more shaded from the sun than other grassland areas, and therefore darker in the DOQQ image. While shadows can affect AISA imagery as well, the spectral indices

help to remove the effects of topography, and are thus less sensitive to topographic differences than the DOQQ images. The ability of the DOQQ to distinguish between tree and grass thus seems to depend to a large extent on tree density and the contrast between the trees and underlying vegetation.

Using the discriminant function analysis, four of the indices had the lowest rate of misclassification when tested with the validation points. The NDVI, GNDVI, VARI, and WDRVI all had a 23.8% misclassification rate (Table 2.1). The EVI and SAVI had the highest rates of misclassification (33.3 %). These results confirm the trends observed when the pixel distributions and classifications are viewed, where the NDVI, VARI, GNDVI, and WDRVI were the most effective indices for separating tree and non-tree cover types, while the EVI and SAVI were the least effective. Because of the poor performance of the EVI and SAVI in this study, they will be excluded from further analyses. The unimodal distributions observed for these two indices are likely caused by the corrections for which the indices were designed. In the case of the EVI, the effect of the background is minimized by applying several correction factors. Because the grassland areas presumably have significant bare ground and standing dead biomass signals, this correction acts to remove what could be a primary difference between the tree and non-tree vegetation types, which is the effect of underlying vegetation. Presumably, tree canopies are large enough and the leaf distribution is localized enough for the signal to be less affected by soil reflectance. For the SAVI, the same sort of situation occurs, where the index is designed to remove the influence of the soil background. The results from these two indices indicate the possibility that the soil reflectance has a significant and important influence on the grassland signal – enough to

make the generalized non-tree signal significantly lower than the general tree signal. The RRDI green index will also be excluded from further analysis because it lacks a true bimodal distribution and is not one of the best indices for separation of tree and non-tree cover types as observed with the discriminant function analysis. Also, it is largely redundant with the RRDI red edge index. Relationships between these indices (EVI, SAVI, and RRDI green) and the ecological variables selected for analysis (such as LAI) are poor. In addition, the removal of these indices will simplify later analyses by reducing the number of regressions that need to be performed between the indices and biophysical variables.

When the Landsat-emulating indices are compared to their AISA counterparts, it is unclear whether there is any advantage to the narrow waveband indices. The Landsat-emulated indices all showed misclassification rates that were identical to their narrow band counterparts (Table 2.1). Because of the identical results, it is difficult to come to any conclusions at this point about the effectiveness of the spectral resolution of the AISA sensor when compared to a Landsat-type sensor. Previous studies by Lee et al (2004) and Schlerf et al (2005) have shown slight advantages to using hyperspectral data over multispectral data for estimation of LAI. However, a comparison of wide band and narrow band data for that relationship was not addressed in this thesis.

An additional variable to consider when investigating the separation of tree and non-tree cover types at a given location involves the signal of the background material, which in this case is predominantly grassland. Because a grassland background is spectrally dynamic (i.e. subject to change temporally), it is important to address the possibility that the signal of the background (when expressed in terms of a vegetation

index value) was especially low due to the time that the image was acquired (August, in this case). The phenology of pine forests is certainly less dynamic seasonally than grasslands, where species have distinct green up and senescence periods that are more easily detected spectrally. Part of the motivation in acquiring the AISA imagery in early August was because of the reduced response of the grassland for indices such as NDVI. Therefore, it is necessary to consider whether phenological changes in the grassland would effect the bimodal distribution of the imagery.

To investigate this issue, AISA images that were acquired on June 26, 2003, at a Sand Hills grassland site (Barta Brothers Ranch) were compared to the AISA images acquired for this project. The distribution of values for the NDVI image at the grassland site shows a more normal distribution with no bimodality (Figure 2.5). Also note the values of NDVI within the grassland image: the peak value is well below the threshold value that separates tree from non-tree. This suggests that the NDVI signal does not increase enough in the grassland areas, even at peak greenness, to affect the threshold that separates tree from non-tree. A closer look at the grassland image provides an interesting counterpoint, however, where the area highlighted in Figure 2.5 shows a slightly higher average NDVI value (app. 0.51) and contains some highly productive subirrigated, or "wet" meadow areas where NDVI is as high as 0.78, well above the threshold established in the BU/NNF NDVI image (Figure 2.5). These wet meadow values are also well above the NDVI values of the small patches of trees present at the grassland site. So, while it seems that typical upland Sand Hills areas do not exhibit a high enough NDVI value to affect the approximate threshold value that separates tree and non-tree classes, areas of high productivity (exemplified by the wet meadows in the grassland image) may have

NDVI values that are high enough to cause misclassification. In portions of the Sand Hills, including the BU/NNF, interdunal valleys are generally dry because of the low water table. In other regions (such as the area where the grassland image was acquired), interdunal valleys contain hay meadows or wetlands that are significantly more productive than upland grasslands. Therefore, while it is unlikely that the NDVI signal in the grasslands at the BU/NNF would be high enough to shift the index distribution from bimodal to unimodal, the time of year at which data is collected should be considered when acquiring imagery or conducting research at the BU/NNF. Such a subject may be useful for further study, where the development of a seasonal NDVI (or other index) curve could improve understanding of the temporal variability in grassland spectral response and/or productivity.

Conclusion

This first order approach at analyzing the AISA imagery gives some indication of the indices' abilities with regards to separating tree cover types from non-tree cover types. In order to analyze tree canopies, it follows that one must be able to distinguish tree canopies from non-tree ground cover types, such as grassland and bare sand. From the original 9 indices chosen, 3 (EVI, SAVI, and the RRDI green) have been excluded from further analysis because of their inability to distinguish tree from non-tree. When the histograms for these indices are viewed, it is obvious that a bimodal distribution is not present. Instead, a normal distribution (EVI and SAVI) or a skewed distribution (RRDI green) is observed. The poor performance of these indices for this project is further proven by the higher rates of misclassification from the discriminant function analysis. The higher rates of misclassification indicate that they are unable to discriminate between

pixels known to be tree and non-tree as effectively as the other indices. In the cases of the EVI and SAVI, their correction for soil reflectance may actually lessen their ability to separate tree cover types from non-tree cover types. With indices that do not correct for soil reflectance, the effect of soil reflectance attenuating the vegetation response may actually improve the bimodality of the distribution, where non-tree areas are more affected by background reflectance, attenuating the signal such that it is significantly lower than the reflectance of the tree cover types, and thus creating a bimodal distribution.

When compared to the DOQ, the indices and the 1st principal component image do a better job distinguishing tree from grassland because the spectral information used in the indices and 1st PCA image is less sensitive to topography and is more sensitive to the spectral differences between tree and grassland, while the DOQ is a grayscale image. The DOQ is more effective than the indices at distinguishing tree from background in more densely forested areas. This is probably due to its higher spatial resolution, where these details are more easily distinguished in the DOQ.

The NDVI, GNDVI, WDRVI (α=0.15), and VARI all show both a bimodal distribution and the lowest rates of misclassification in the discriminant function analysis, leading to the idea that these indices are the best choice for further analyses. However, no definitive statements can be made about the superiority of a given index because their strengths and weaknesses have not been fully investigated. NDVI, for example, loses sensitivity to biophysical parameters such as LAI and pigment concentration at high vegetation densities. This study was not set up to test these weaknesses, so further analysis is necessary. It is also difficult to make any decisions regarding the utility of

narrow wavebands that instruments such as the AISA sensor provide. No differences were observed between the Landsat-emulated indices and the short-waveband indices, so no conclusion can be made at this time about whether the small waveband indices improve utility.

Comparison of results from this study with AISA imagery obtained earlier in the growing season at a grassland site suggests that the seasonal variability expected for NDVI in upland Sand Hills grasslands is not large enough to change the essentially bimodal distribution observed for tree versus non-tree pixels. However, highly productive locations in the Sand Hills such as wet hay meadows and wetlands have high NDVI values that, in some seasons, may exceed values observed for pine or cedar vegetation.

The data from this study indicates the seasonal variability of the NDVI signal in the non-tree cover type at the BU/NNF is not likely to reach a high enough level where the bimodality of the distribution within the scene is affected. However, to test this hypothesis and generalize this approach for wetter areas of the Sand Hills, further study is necessary.

Figure 2.1 The images below show the flightline after the application of the vegetation indices. To the right of each image is the histogram of the pixel values for each index. The images in the left column are the regular indices, while those on the right use the Landsat-emulated indices. The threshold value is shown in the box above the histogram. In these images, the contrast of reflects the value, where a higher value is lighter in shade than a lower value, so that high values are white, while dark values are black.

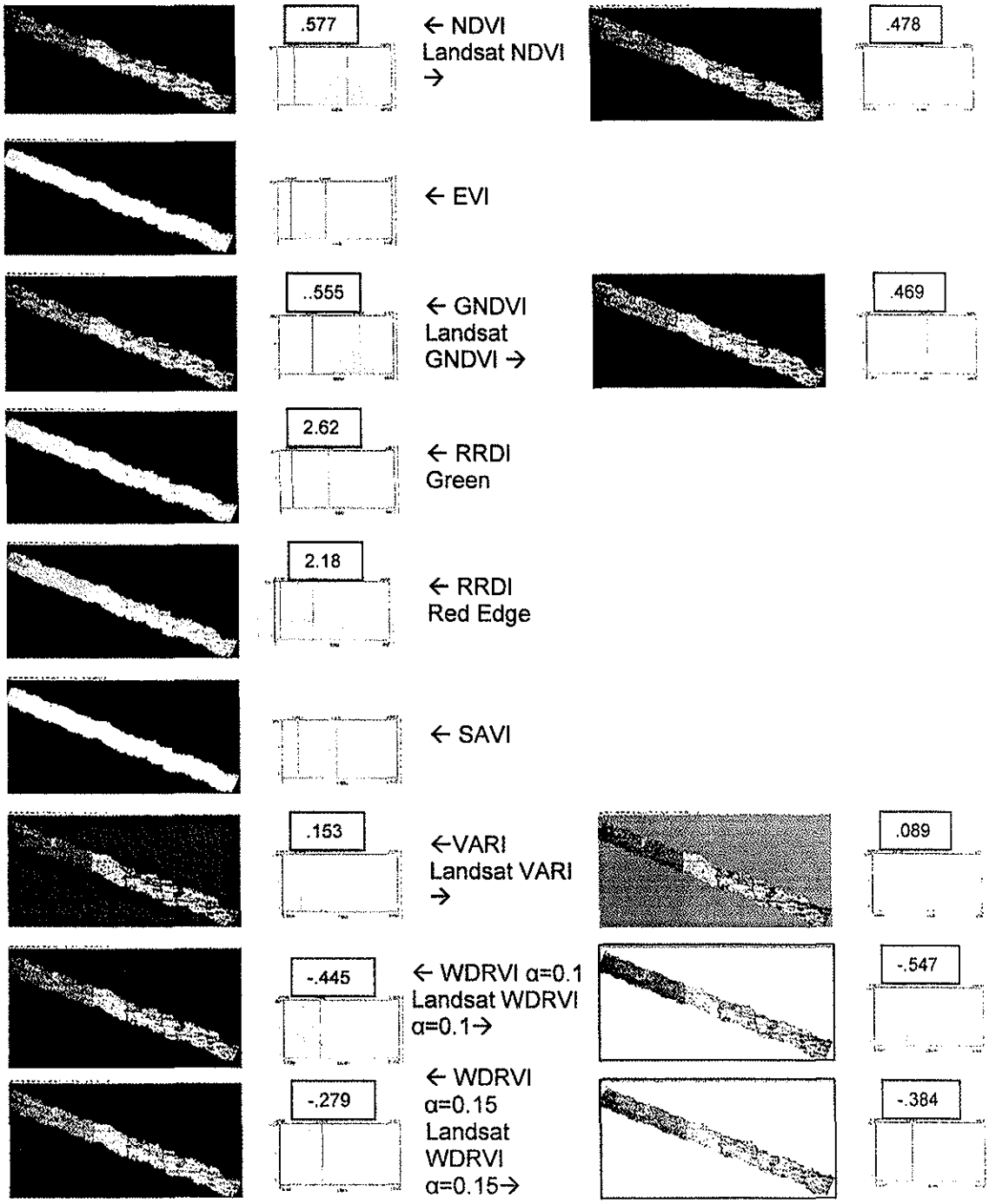

Figure 2.2 The 1st two classified principle component images are shown along with the histogram distributions of the pixels and the value used to set the threshold between tree and non-tree cover types. The third image is the classified NDVI image presented for comparison with the principle component images. Dark green represents tree in the images, and tan represents non-tree cover types.

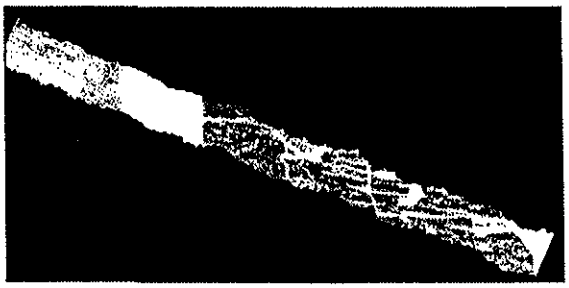

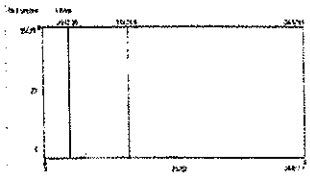

Threshold value = 10552.2

PC1

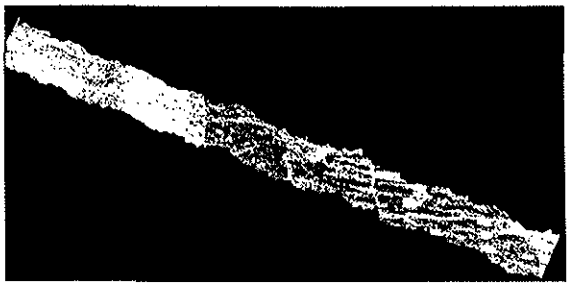

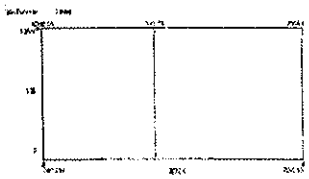

Threshold value = -530.767

PC2

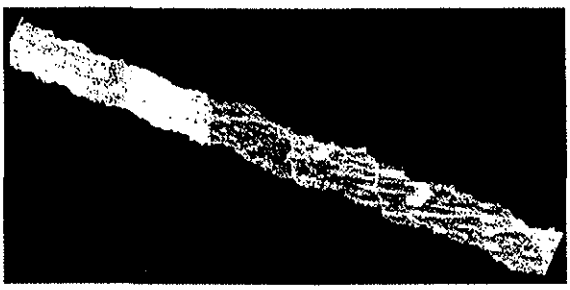

NDVI

Figure 2.3 The top image is a grayscale AISA image. The white box reflects the approximate area shown below in the two grayscale images, which reflect the tree/non-tree classification according to the VARI and NDVI vegetation indices. In these image, light tones indicate the non-tree class and dark tones indicate the tree class. The VARI binary image separates cedar and grassland areas more effectively than the NDVI image. Note especially areas highlighted with ovals, where the VARI does a much better job of classification than the NDVI.

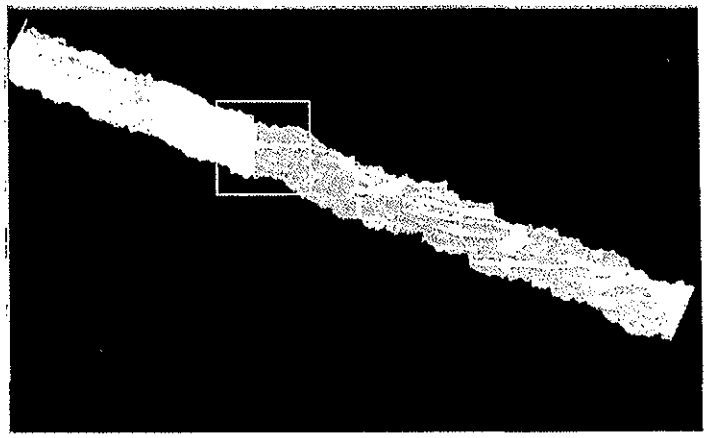

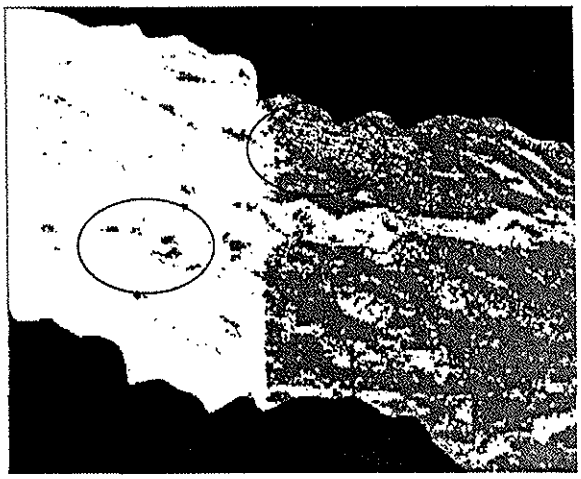

VARI NDVI

Figure 2.4 The DOQQ was subset with the area of the flightline. The resulting image was bimodal, so the threshold value (82.32) was applied, and the resulting classification on the right was produced. The closeup view was then compared to the NDVI classified image (tree in green, non-tree in tan). Notice the large differences in the grassland and forested areas between the DOQQ and NDVI images.

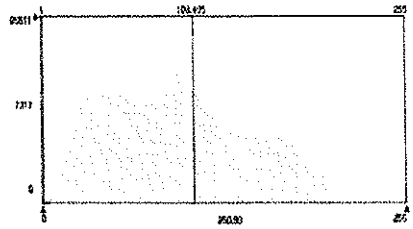

Bimodal distribution of DOQQ

Subset DOQQ

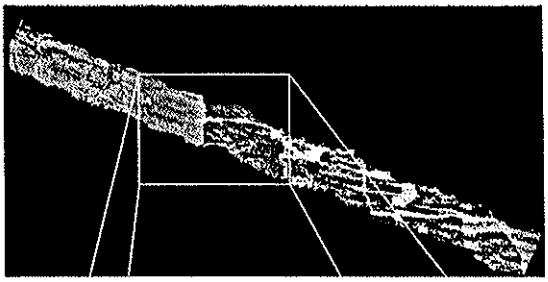

Classified DOQQ

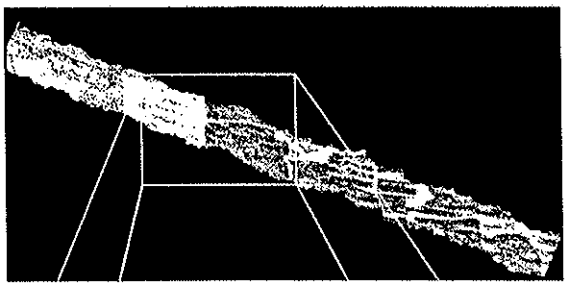

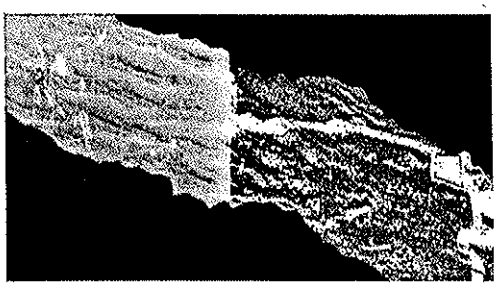

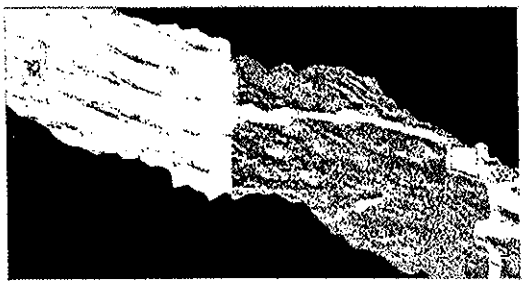

NDVI

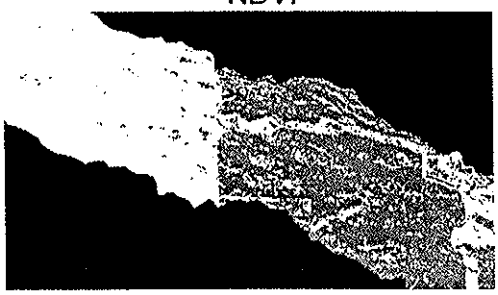

Figure 2.5 NDVI images of the BU/NNF and the Barta Bros. ranch (a grassland area) are shown with histograms of the pixel distributions. Note the bimodal distribution of the NDVI image and the unimodal distribution of the BBR image. The threshold value for the NDVI image (0.577) is represented by the red line on all the histograms.

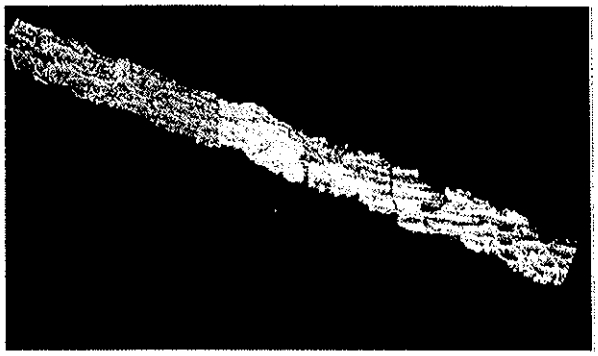

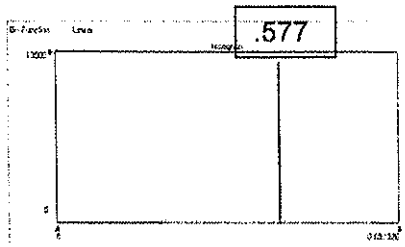

The approximate values for the peaks in this histogram are 0.434 (left) and 0.708 (right)

June 26, 2003 AISA image – the area outlined in white is expanded below

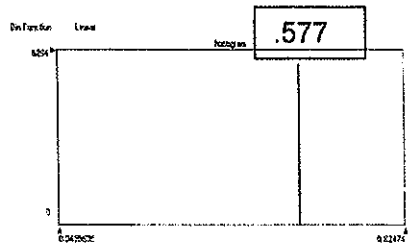

The approximate value for the peak of this histogram is .44

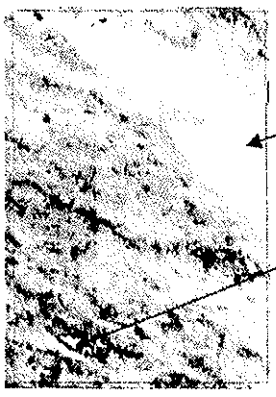

Wet Meadow (highly productive area – NDVI app. 0.7

Eastern Red Cedar patch – NDVI app. 0.55

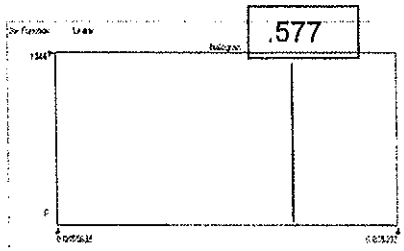

The approximate value for the peak of this histogram is .516

Table 2.1 A summary of the performance of each index from the discriminant function analysis. The rate of misclassification (%) is shown for each index.

Index	% misclassified
NDVI	23.8%
GNDVI	23.8%
EVI	33.3%
RRDI_G	28.6%
RRDI_RE	28.6%
SAVI	33.3%
VARI1	23.8%
VARI2	23.8%
WDRVI (0.1)	28.6%
WDRVI (0.15)	23.8%
L7_NDVI	23.8%
L7_GNDVI	23.8%
L7_VARI	23.8%
L7_WDRVI (0.1)	28.6%
L7_WDRVI (0.15)	23.8%

Chapter 3

Estimation of LAI Using Hemispheric Camera and Ceptometer Optical Methods

Introduction

Although the long-term goal of researchers and managers may be to describe the canopy structure of forests and woodlands with remote sensing, their work nevertheless begins on the ground. The goal of this portion of the study is to evaluate the effectiveness of a hemispheric image-producing LAI camera system for analyzing open wooded ecosystems like those found at the BU/NNF. Leaf Area Index will be used as a measure of stand structure because it is a key parameter in understanding several plant processes, such as evapotranspiration, photosynthesis, yield, and radiation exchange with the atmosphere, and because its use is well-documented (Gower and Norman, 1991; Law, et al., 2001; Baret and Guyot, 1991; Price and Bausch, 1995). Also, equipment is commercially available for non-destructive measurement of LAI from the ground.

Even though LAI is a widely used measure of tree canopies at spatial scales ranging from individuals to grid cells in global ecosystem models, considerable ambiguity exists in defining and measuring LAI. The most precise method of measuring LAI for a particular tree species or vegetation type involves the destructive harvest of replicate trees, followed by measurement of actual leaf area for subsamples of the canopy. When combined with biomass measurements of leaves, boles (trunks), bark and branches, destructive harvests allow development of species- and site-specific allometric equations that predict aboveground biomass, canopy LAI and other stand attributes given simple measures of tree diameter (DBH) and height (White, et al., 1997; Gower, et al., 1999; Nemani, et al., 1993; Gower and Norman, 1991; Law, et al., 2001; Turner, et al.,

1999). This approach is very labor intensive, and current research on forest canopies and carbon balance relies on surprisingly few published allometric relationships. The basic utility of optical measures of LAI lies in their non-destructive nature. Most studies utilizing ground measurements of LAI rely on optical measures from instruments such as the LiCor LAI-2000, ceptometers that measure gap fraction, or hemispheric images taken from cameras fitted with fisheye optics (Law, et al., 2001; Gower and Norman, 1991; Gong, et al., 1995). It is also important to stress that LAI estimates from destructive harvests and non-destructive optical methods are generally not equivalent. Optical methods actually measure "plant area index", since both leaves and non-photosynthetic tissues (e.g. branches) obstruct light, but these values are often referred to as LAI in the literature. The utility and accuracy of different LAI measurements is, unfortunately, context dependent and changes for different research and management applications.

Optical measurements of LAI all rely to some extent on assumptions about the structure and distribution of the leaves, shoots, and/or branches. These assumptions include random orientation of leaves and branches, no transmission of light through leaves, and small leaf size relative to the field of view (WinSCANOPY manual, 2002). In pine canopies, because leaves are highly organized at the leaf and shoot levels, the assumptions of random orientation at leaf and branch levels are violated (Gower, et al., 1999). Law, et al., 2001 provides an excellent synopsis of some methods used to overcome these errors. For correction of clumping at the leaf scale, the ratio of total needle projected area / mean projected shoot silhouette area was used (Gower and Norman, 1991; Oker-Blom and Smolander, 1988; Stenberg, 1996). In the Law, et al.

study, the following equation was used to correct for clumping of needles within the shoot, at scales larger than the shoot, and interception by woody biomass:

$L_{hc} = (1-\alpha)L_e \times \gamma_E/\Omega_E$

where L_{hc} is the half total surface area (m^2) of needles per m^2 of ground, α is the woody-to-total area ratio, L_e is the effective leaf area (includes woody component), γ_E is the total needle projected area / mean projected shoot silhouette area ratio, and Ω_E is an index value that quantifies the effect of clumping at scales larger than the shoot (Law, et al., 2001).

While it is important to understand the utility and limitations of these instruments for measuring LAI, the goal of this chapter was not to validate non-destructive LAI estimates against clipping or allometric estimates. In the study of LAI, one soon realizes "truth" is elusive; all estimations rely on assumptions. Rather, the goal is to fully understand the utility of the hemispheric camera system and its ability to detect ecologically significant differences in canopy structure.

Previous research at BU/NNF established a series of 20 plots that represent a range of cover types from open grassland to closed canopy forest (Ding, 2002). Wedin et al. (unpublished) proposed that a threshold exists for canopy cover above which the function of the forest changes. Stable carbon isotope samples were taken from each of 20 plots located within the BU/NNF. These plots were chosen according to canopy cover, so that a a range of cover types from open grassland to closed canopy forest were included. When these C isotope values were compared with ponderosa pine basal area measured in each of these 20 plots, a threshold emerged along the basal area gradient at approximately 20 m^2/ha., above which C_4 grasses were essentially excluded (Figure 3.1).

The impacts of a change from C_4-dominated grasslands and savannas to C_3-dominated forests are diverse and may include decreased soil moisture and ground water recharge, reduced forage production for livestock and wildlife, decreased soil organic matter, and increased fuel loads that contribute to altered wildfire behavior. The goal of this chapter is to develop an easily used, non-destructive measure of LAI that can accurately assign relatively small areas to their appropriate position along this ecologically significant gradient of pine canopy cover.

Methods

Data was collected at the Bessey Unit of the Nebraska National Forest (BU/NNF) located near Halsey, Nebraska. The BU/NNF is a 25,000 ha unit, of which app. 10,000 ha contain trees. The forested areas contain predominantly ponderosa pine (*Pinus ponderosa)* and eastern red cedar (*Juniperus virginiana)*, which were planted in the early 1900s. Within these forested areas, canopy cover can be highly variable as a result of planting history, past wildfires, and topography, which affects water availability and resource distribution. The grassland areas contain native Sand Hills prairie dominated by grasses including little bluestem (*Schizachyrium scoparium*), prairie sand reed (*Calamovilfa longifolia*) and junegrass (*Koeleria cristata*), and the low shrubs leadplant (*Amorpha canescens*), yucca (*Yucca glaucifolia*), and wild rose (*Rosa arkansana*), with occasional patches of taller shrubs such as wild plum (*Prunus Americana*). 18 of the 20 40 m x 40 m plots were used in this study, along with 3 additional plots that were added later, creating a set of 21 plots designed to cover the range of canopy heterogeneity at the BU/NNF. Measurements were taken in 21 40 m x 40 m plots, which were divided into 16 subplots each (Figure 1.3). Two methods of LAI estimation were used in the 40 x 40

m plots selected at the BU/NNF. The first method utilized an AccuPar ceptometer (Decagon, Pullman, WA), which utilizes a linear array of 80 sensors that measure photosynthetically active radiation (PAR) (between 400 and 700 nm) incident upon the sensor array.

At the BU/NNF, ceptometer measurements were taken in every 10m x 10 m subplot within the 40m x 40m plots in August, 1999. These measurements were initiated on cloud-free days between 10:00 am and 2:00 pm solar time to minimize the effects of sun position on light transmission through a canopy. Measurement of a subplot consisted of a reference measurement outside the plot in an area of full sunlight and measurements in the four cardinal directions from the center point of the subplot. This allows the measures within the canopy (where leaves obstruct some portion of incoming sunlight) to be referenced to the measures of full sunlight (no light intercepted) for calculation of the ratio of light intercepted to total light available. The ceptometer was set to average each of the four center subplot measurements automatically. The ceptometer calculates LAI by inverting a light transmission and scattering model that relies on a leaf distribution parameter, a measure of the zenith angle of the sun, and the extinction coefficient for the canopy.

The second method of LAI estimation, a hemispheric camera system, consisted of a Nikon CoolPix 995 3.34 megapixel digital camera fitted with a Nikon fisheye lens that captured digital images from which LAI could be estimated. The fisheye lens allows for a hemispheric field of view (facing upward) so the entire canopy above the camera can be analyzed. The camera is placed in a device that allows the camera to self-level, so that camera orientation is consistent between successive photographs. Images were acquired

at approximately 60 cm above ground level, so that any forbs and grasses present within the plot are excluded from the LAI estimation. For each measurement, slope and aspect were recorded, as some of the analyses require these variables as inputs. Photos were taken in half of the subplots within the 40m x 40m plots for each of the 21 plots that contained tree canopy cover. The eight subplots in which photos were taken were consistent between plots (Figure 1.3).

The software used for image analysis, WinSCANOPY (Régent Instruments, Inc., Quebec, Canada) is designed for canopy analysis, including calculations of LAI. The calculations of LAI are based on a form of the Beer-Lambert law involving the transmission of light at a given angle as a function of the extinction coefficient at that angle and the LAI. A darkness threshold value must be set on the image where, when shifted to a binary black and white image, canopy is represented as black and background is represented as white. The software then estimates the light transmission (as represented by the white background) and the extinction coefficient within each successive canopy ring which representing a given angle. The software then inverts the equation to estimate LAI (WinSCANOPY manual, 2002). The extinction coefficient is a function of path length, leaf density, and leaf orientation. Because the probability of extinction is greater for the outer canopy rings (at lower angles from the horizon and at much longer path lengths), each successive ring moving towards the center is weighted incrementally so that the presence of canopy within inner rings results in a greater LAI value than would the presence of canopy within outer rings. Examples of the camera images and subsequent analysis can be viewed in Figure 3.2.

The WinSCANOPY software calculates four different LAI estimates. The first, called the Bonhomme and Chartier method, assumes that at the 67.5° elevation angle, gap fraction is insensitive to leaf angle and is related to LAI by a logarithmic function. This method is fast and easy to calculate, but it is less precise than the other methods, as it is very sensitive to what is present in the elevation span (67.5° + or – 5°), while information outside the span has no effect on the estimation (WinSCANOPY manual, 2002).

The second method, called the LAI-2000 original method, simulates the methods used by the LiCor LAI-2000 Plant Canopy Analyzer, an instrument which is often used as an optical method of LAI estimation. This method uses a linear regression to relate LAI to gap fractions at different elevations using 5 elevation rings. The third method is similar to the LAI-2000 original method, except that the number of elevation rings can be chosen by the user. Both of these methods use topographic slope as an input to determine path length, since changes in slope can have an effect on path length. For this study, the default of 20 rings was used for the analysis.

The fourth method, the Ellipsoid-Campbell method, assumes that leaf area density distribution is ellipsoidal in nature for real canopies and uses a nonlinear elimination curve to relate LAI to gap fraction (WinSCANOPY manual, 2002; Campbell, 1986). This method was developed to address an assumption of most indirect methods of LAI estimation that leaf orientation distribution in azimuth is random. Real canopies are better represented by distribution models that assume other distributions, such as horizontal (planophile) dominant, vertical (erectophile) dominant, or spherical and

ellipsoidal models, which assume the area orientation distribution is best represented by a sphere or ellipsoid (WinSCANOPY manual, 2002).

To deal with the problems associated with the nonrandom distribution of leaves in coniferous canopies, the WinSCANOPY software calculates two LAI estimations for each of the methods listed above: the standard "linear" method, and a "log-average" method that averages the logarithms of the individual gap fractions for each elevation ring, as described by van Gardingen et al. (1999). The log-average method reduces the underestimation of LAI in nonrandom canopies such as pines. Both methods were compared in this study.

While the goal of both ceptometer (with Accupar software) and the hemispheric lens (with WinSCANOPY) is to estimate leaf area index, it is unclear how comparable the results from these instruments are. These two instruments derive LAI from different methods. A ceptometer uses a linear array of photodiodes that measure photosynthetically active radiation (PAR) between 400-700 nm. To estimate LAI, it uses an inversion of transmitted PAR. The camera system takes a hemispheric image and estimates gap fraction at different elevation angles, then uses an inversion of gap fraction to estimate LAI. Neither system can distinguish between photosynthetic and non-photosynthetic vegetation, so woody material may be counted erroneously as leaf area. To clarify this point for further discussions, when results from these LAI estimations are referred to as "LAI," they are in reality measuring "plant area index," which includes non-photosynthetic vegetation. The potential implications of this discrepancy between plant area index and LAI will be discussed later. To evaluate the effectiveness of the camera system used in this study, the LAI estimates from the camera system will be

compared to estimates taken with an AccuPAR Linear PAR/LAI ceptometer, model PAR-80.

Because both LAI estimation and measurement of reflectance from remote sensing platforms are indirect measures of canopy cover, basal area, tree density, and pine litterfall measurements were used as direct measures of stand structure. Existing data for these plots provide a relatively complete characterization of canopy structure, particularly at the closed-canopy end of the canopy cover gradient (see Ch. 1, Ding, 2002). These direct measures were compared with LAI to determine whether a relationship exists between the indirect measures (LAI) and the direct measures listed above. The diameter at breast height (DBH) was measured for every tree within every subplot for all 21 plots that contained forest cover. These DBH measures were then converted to basal area, which, when averaged on a subplot basis, gives an indication of the size and productivity (wood volume) within a subplot. Tree density in each subplot was converted to number of trees per hectare. Basal area was a strong correlate of numerous parameters (such as grass or forest floor biomass) across the canopy cover gradient (Ding, 2002; Figure 3.3). Basal area also integrates both size and number of trees at the plot or subplot scale. Therefore, it will be used as the directly measured variable most representative of the canopy cover gradient for comparison with LAI estimations.

To reduce the number of permutations that must be done for any given analysis, the eight LAI estimation methods from the camera (four linear and four log-averaged methods) were analyzed to determine which method would be used for further analysis.

Each estimation method was compared to basal area for each of the 8 subplots within 21 plots.

After the optimal LAI estimation method for the camera was selected, the camera method was compared to the ceptometer LAI estimation method to determine which method is more effective for estimating LAI in this study. The coefficient of variation (CV) was calculated for the plot averages of each method. The coefficient of variation is a measure of relative scatter with respect to the mean, or a measure of deviation of a variable from its mean. So, when calculated for the LAI measures, it gives an indication of the scatter within a plot with respect to the plot mean.

Finally, basal area was regressed against LAI. Both individual measures and plot averages of basal area and LAI were compared. To test the ability of the LAI camera system to estimate the cover of an area in terms of basal area, regressions were performed with different numbers of randomly selected subplots from each plot. The goal of this particular analysis was to understand how many measurements with a hemispheric lens are necessary to adequately estimate LAI within a 40 m x 40 m plot, and if that number changes as stand structure changes. This process consisted of selecting 2 sets of n (n=1, 2, 3, or 4) subplots randomly and then averaging LAI values to obtain two estimates of average LAI for each plot. Since LAI measurements were only taken in 8 subplots, when n=4 subplots, all of the subplot LAI measurements taken in a plot were used. Thus, the first iteration of this experiment compared the average basal area for each plot with 2 randomly selected subplots from each plot. The second iteration compared the average basal area for each plot with 2 sets of 2 randomly selected subplots. The third and fourth iterations compared average basal area per plot with 2 sets of 3 and 2 sets of 4

randomly selected subplots, respectively. The goal with these four iterations was to maintain the same overall sample size between iterations while investigating the ability of the LAI to determine canopy conditions through the averaging of multiple readings.

Results and Discussion

When the camera LAI estimations were regressed against basal area, the Ellipsoid-Campbell (E-C) method showed the highest R^2 (0.55), though the values for the two LAI-2000 methods were not much lower (0.548 for the LAI-2000, 0.541 for the LAI-2000 generalized) (Figure 3.4). The E-C method also had the highest R^2 (0.516) value among the log-transformed LAI values, though the R^2 values were uniformly lower for the log methods than the linear methods. While this might suggest that the linear methods should be selected over the log-transformed methods, the theoretical background for the log-transformed methods suggests that these LAI estimations are more appropriate for the pine woodlands at the BU/NNF. LAI estimations are underestimated in coniferous canopies as a result of highly organized shoots. The log-transformed method applies a clumping compensation method that was designed for non-random or discontinuous canopies, such as those of a coniferous forest (WinSCANOPY manual, 2002). The effects of the log method are seen when the range of LAI values is compared between the linear and log methods. The range of LAI values increased by as much as 47% for the E-C method, where LAI ranges from 0 to 2.2 with the linear method, but is widened to a maximum of 3.25 with the log-averaged method. While the linear LAI estimates averaged less than 2.0 for the dense pine stands, the log-transformed estimates averaged 2.3 (E-C method). While this log method increases the variability (and consequently, may reduce the strength of some correlations), it improves the range of

LAIs such that our results are coincident with several studies that see a maximum LAI between 3.0 and 4.2 in coniferous canopies, with pines at the low end of the range (Boyd, et al., 2000; Chen and Cihlar, 1996; Fassnacht, et al., 1997; Fernandes, et al., 2002; Hu and Miller, 2000; Law, et al., 2002). Approximations of stand LAI from existing data for these plots suggest LAI for the high density plots lies between 2.0 and 3.0 (see Chapter 1). For this reason, the E-C log-transformed method was the primary estimation method chosen for further analysis.

A regression between the two LAI estimation methods (ceptometer and camera) for every subplot shows a fairly messy relationship ($R^2 = 0.42$, slope = 0.33, Figure 3.5). When the values for each method (ceptometer and E-C camera log-averaged methods) were averaged over the entire plot and compared, the regression line had a slope of 0.63 with an R^2 of 0.75 (Figure 3.6). The two methods predicted similar LAI values in dense plots, while differing considerably in their predictions for sparse, savanna plots. When the coefficient of variation for each LAI method was plotted against basal area, the hemispheric camera method showed a lower CV for every plot in the study. This indicates the hemispheric LAI system is a more effective method for capturing the variability of the plots sampled because when compared directly with the ceptometer system, the camera had a lower standard deviation with respect to the mean, and this relationship was constant through the entire gradient of canopy covers.

The distribution of LAI within the plots shows how spatially heterogeneous an area of woodland can be. Generally, the subplots within the dense plots are much more similar than the subplots within more heterogeneous areas. As shown in Figure 3.7, as the average LAI within a plot decreases, the standard deviation of subplot LAI within a

plot increases. The more heterogeneous plots may have individual subplots that have a similar LAI value to some of the more dense plots, but on an individual subplot basis, the camera method seems unable to capture the variability of the entire plot by only measuring a single subplot. This is likely due to the camera system, which is more sensitive to canopy directly above it than to trees on the periphery of the viewing area. Thus, the proximity of the camera to an individual tree can have a large effect on the LAI estimation. In a dense plot, this is not a significant problem, since the proximity to the nearest tree is always close. In the more heterogeneous plots, where trees are much more scattered, more measurements are necessary to capture the entire range of LAIs that could be estimated by the camera. In these heterogeneous plots, the possibility exists that a single point measurement would occur either directly under a tree or in an area large enough that trees are only detected on the periphery, leading to a misrepresentation of the canopy LAI within that plot.

LAI was compared to basal area and tree density for all subplots and plots to determine how well a measure of basal area can predict LAI. For a first order analysis, no averaging of any values was done. LAI increased linearly as basal area increased (R^2 = 0.516, Figure 3.8). However, the relationship is not particularly strong, and for any given basal area, LAI can fluctuate by as much as 2. When all measures were averaged over the entire plot, the fit improved drastically (Figure 3.8). As basal area increases, LAI increases non-linearly, though no asymptote seems to be reached at the highest basal area measured. While this relationship is quite strong, it may not be necessary to take as many as 8 subsamples in a 40 m x 40 m area to estimate the LAI of the area.

To determine how effective the camera system is for estimating LAI in the plots, the coefficient of variation (CV) was calculated on the LAI data for each plot (Figure 3.9). The dense, more heterogeneous plots (containing higher basal area) have a low CV, indicating that most of the measurements do not differ significantly from the mean, while the more heterogeneous plots have high CV values indicating that an individual measurement may differ greatly from the mean. So, if the cover in an area is heterogeneous, more readings are necessary to adequately describe the area in terms of LAI. Above a basal area of approximately 25, the CV value is relatively low, indicating fewer measurements are needed to adequately capture stand variability.

The analyses discussed thus far treated basal area as the independent, or known variable, and LAI as the dependent, or experimental variable in regressions. However, the goal of this study is to understand the ability of the LAI measuring systems, particularly the hemispheric lens, to quickly and accurately predict stand attributes when they have not been measured. In other words, basal area becomes the unknown or dependent variable. The analyses using four different iterations of randomly selected subplots were designed to further investigate how effectively the camera system can capture the range of variability within the 40 m x 40 m plots. As Figure 3.10 shows, the first iteration (2 sets of 1 subplot) showed an R^2 of 0.62. The second iteration (2 sets of 2 subplots) showed an improved R^2 (0.68) and a tighter confidence interval. This trend continued with the third iteration (2 sets of 3 subplots) where the R^2 increased (0.83) and the confidence interval tightened. The final iteration (2 sets of 4 subplots) exhibited a lower R^2 (0.77) than the third iteration, indicating negligible or diminishing returns with

calculations based on the data collected in the dense pine stands at the BU/NNF suggest that their "true" LAI value lies between 2 and 3 (see Chapter 1). This is consistent with the log-transformed LAI estimates in this study from WinSCANOPY (e.g. the hemispheric lens), as well as estimates from the Accupar ceptometer. In low density, savanna stands, the two instruments gave quite different estimates. Which is better? The answer is context dependent. While the ceptometer probably does a better job of characterizing the radiation regime at a point (e.g. habitat for a particular plant or animal), the hemispheric lens samples a relatively large area in open woodlands (>10 m) and thus gives a better picture of average canopy conditions.

The caveat to this conclusion, however, is that single camera measurements are inadequate. If the observer knew a stand was uniformly dense, one measurement might be sufficient. However, this presupposes data on canopy structure has already been collected, which defeats the purpose of the hemispheric lens as an efficient tool for surveying and describing canopies. To describe canopy density in terms of LAI in pine woodlands, at least 3 measurements spaced approximately 15 m apart or further are recommended based on this study. This finding is coincident with Walter and Himmler (1996) who found measurements with a camera system similar to the one used in this thesis to be spatially autocorrelated up to about 10 meters in a Scots pine-dominated forest. Therefore, any measurements taken less than 10 meters apart are not independent.

The camera has other capabilities that extend beyond what was used in this portion of the experiment that may enhance both the ability of the camera system to estimate LAI and the ability to characterize the light and canopy environment of a given point. For example, the camera is able to perform what is essentially a supervised

classification on imagery to determine LAI. With this method, points are chosen within the image that reflect the different colors present, such as canopy (typically green), non-photosynthetic vegetation (brown or black), and background (blue or white). While this method is more time intensive than the black and white image method used in this thesis, it may aid in eliminating the non-photosynthetic vegetation influence on the estimated LAI value, and as such may be a valuable tool. Further study is needed to evaluate this possibility.

Figure 3.1 Stable carbon isotope data from Wedin, et al (unpublished) shows a shift in grassland species composition between a basal area of 15-20 m^2/ha.

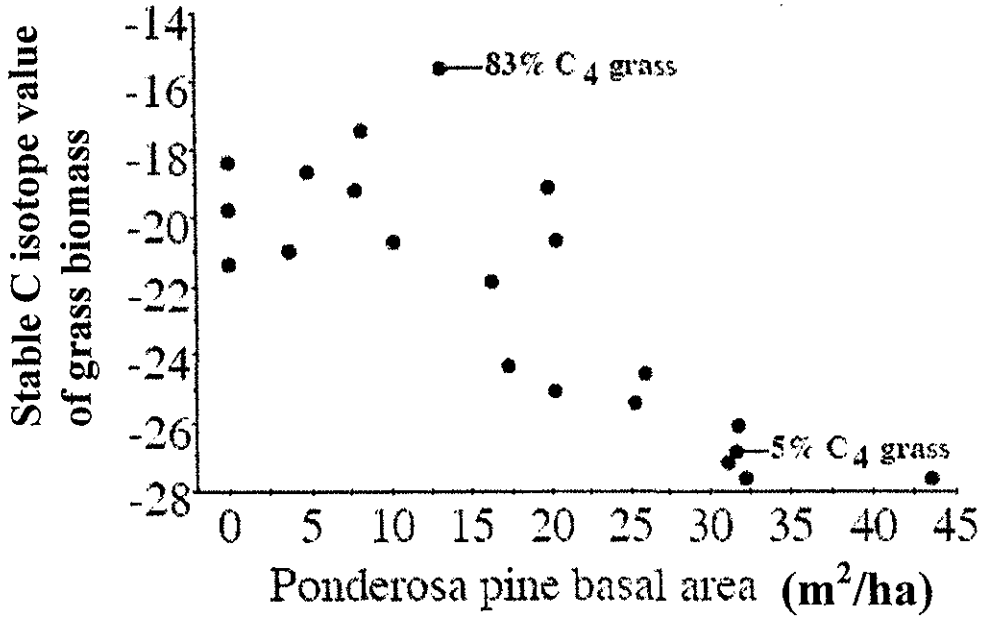

Figure 3.2 Images taken with the hemispheric camera are shown on the left. To the right, the black and white images show how canopy is characterized by the software (canopy in black)

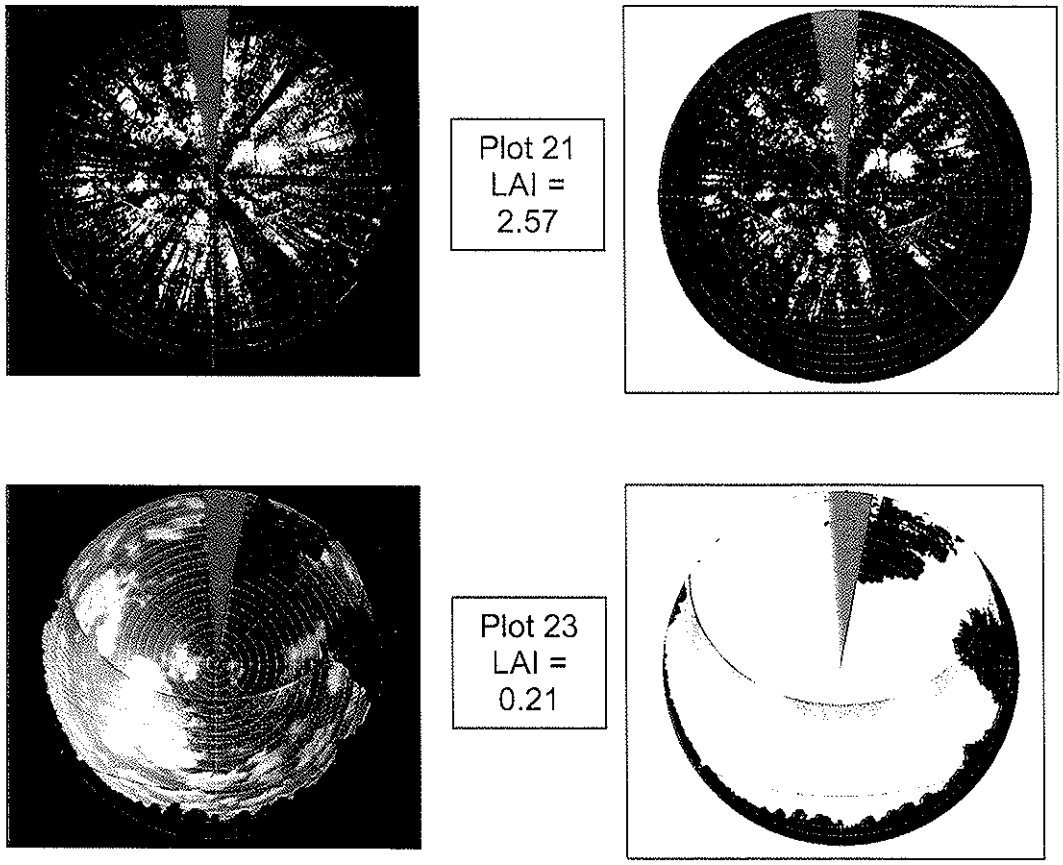

Figure 3.3 Basal Area (X-axis) is plotted against grass biomass (g/m^2), Forest Floor biomass (g/m^2), and tree density (trees/ha). Data from Ding, 2002.

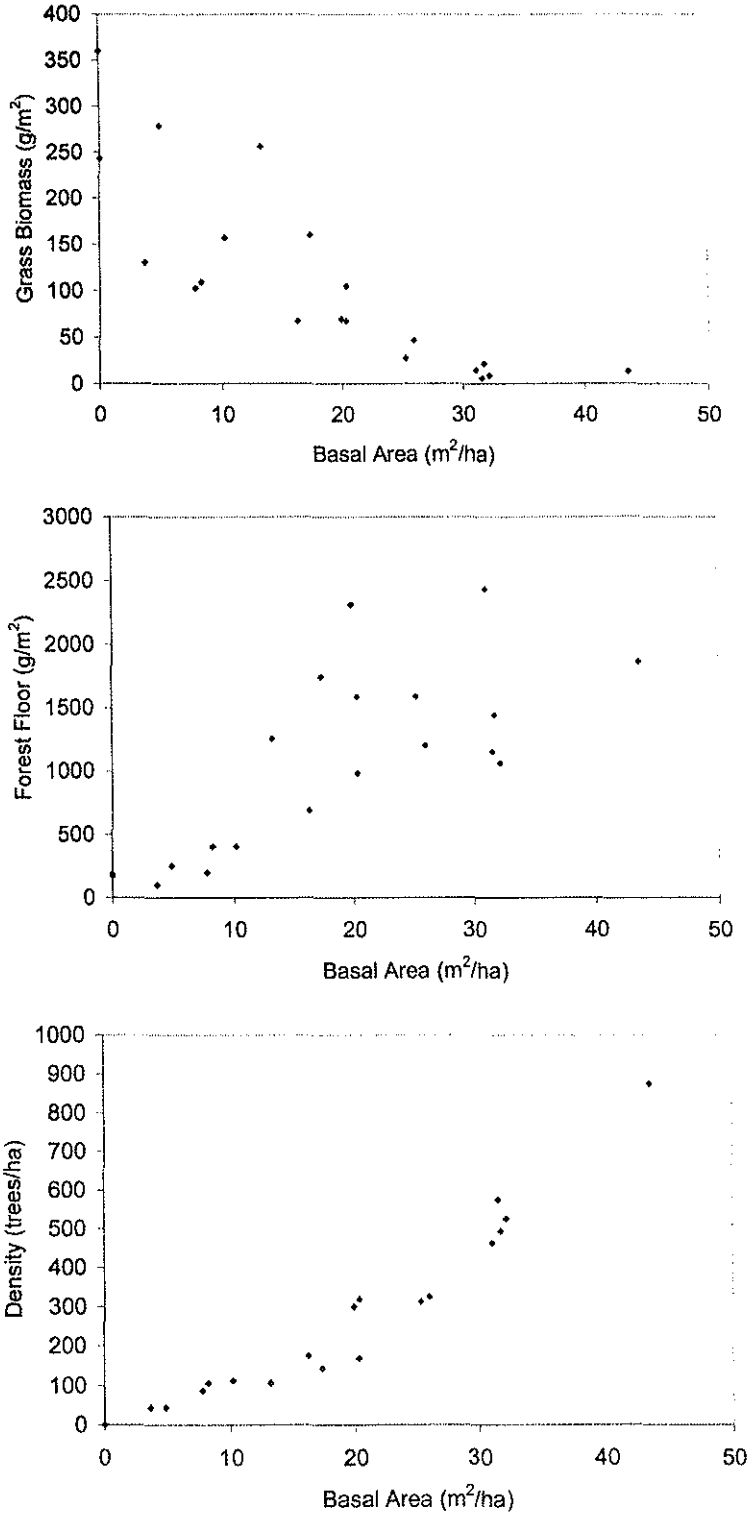

Figure 3.4 Basal area and LAI regressed for all 8 LAI methods (4 Lin and 4 Log). All relationships are significant at p< 0.001

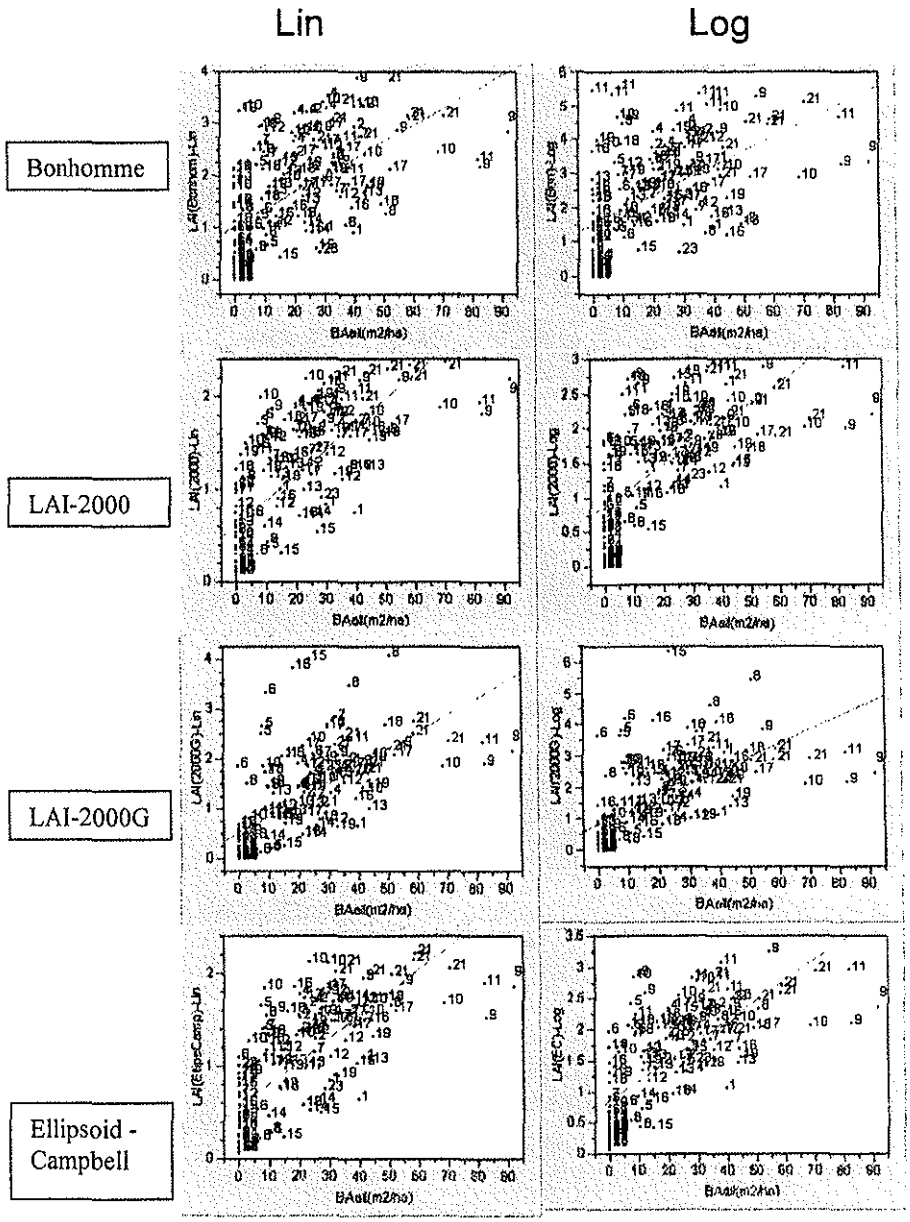

LAI	Lin	Log
Bonhomme	.35	.31
LAI-2000	.53	.44
LAI-2000g	.47	.41
Ellipsoid-Campbell	.54	.52

Figure 3.5 Comparison of camera LAI estimation (ordinate) and ceptometer LAI estimations (abscissa). All relationships are significant at $p < 0.001$

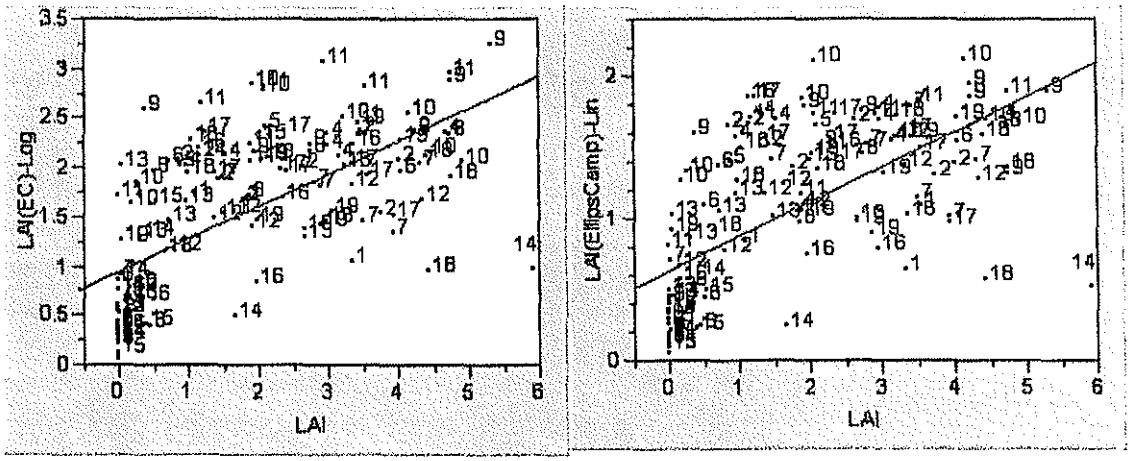

	Lin	Log
R^2	0.42	0.43

Figure 3.6 Linear and logarithmic LAI estimation methods (ordinate) regressed with ceptometer LAI estimations (abscissa). Values are averaged for the whole 40 m x 40 m plots. All relationships are significant at $p<0.001$

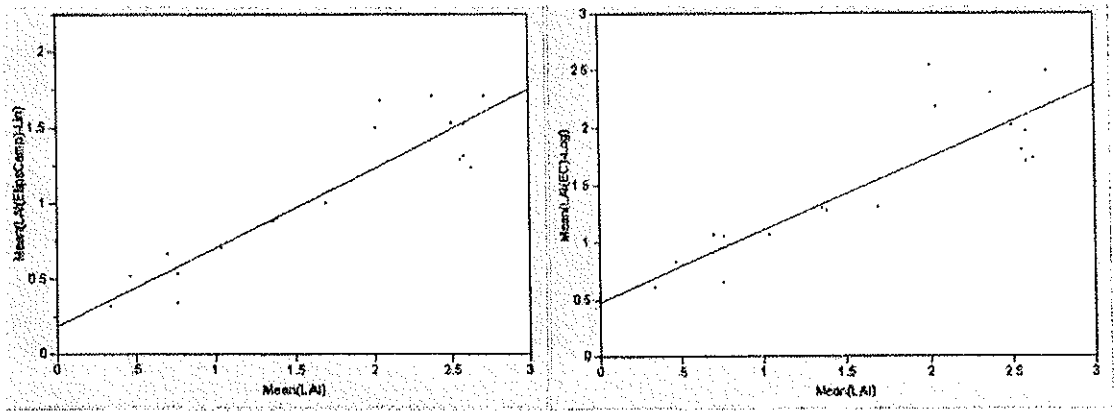

	Lin	Log
R^2	0.84	0.75

Figure 3.7 Camera LAI estimations within the plots are plotted from left to right by average LAI within the plot. The standard deviation of LAI within each plot is shown on the bottom
graph.

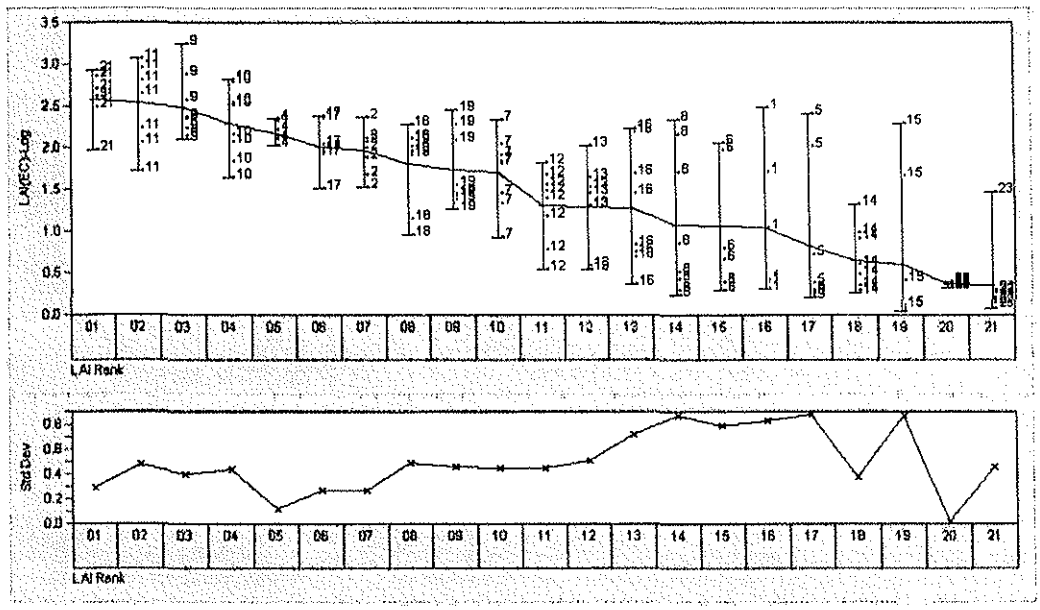

Figure 3.8 Basal area and camera LAI estimation regression with no averaging of values on the left. On the right, the same variables are plotted, but the measurements have been averaged by plot. Relationships are significant at $p<0.001$.

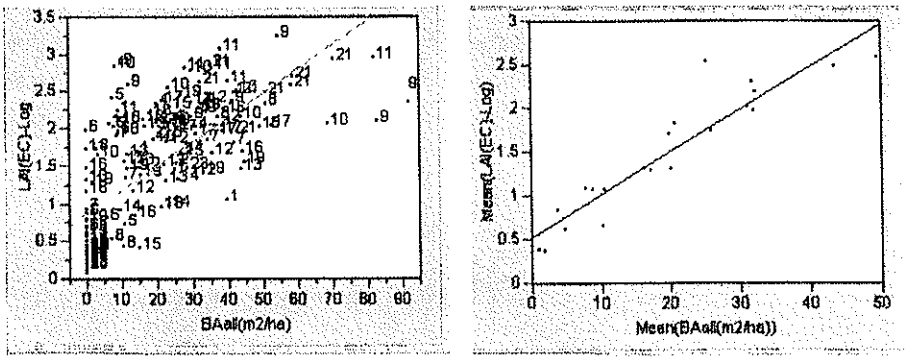

	No Averaging	Avg. by Plot
R^2	0.516	0.906

Figure 3.9 The Coefficient of Variation was calculated for the camera LAI estimations, then plotted against the mean basal area values

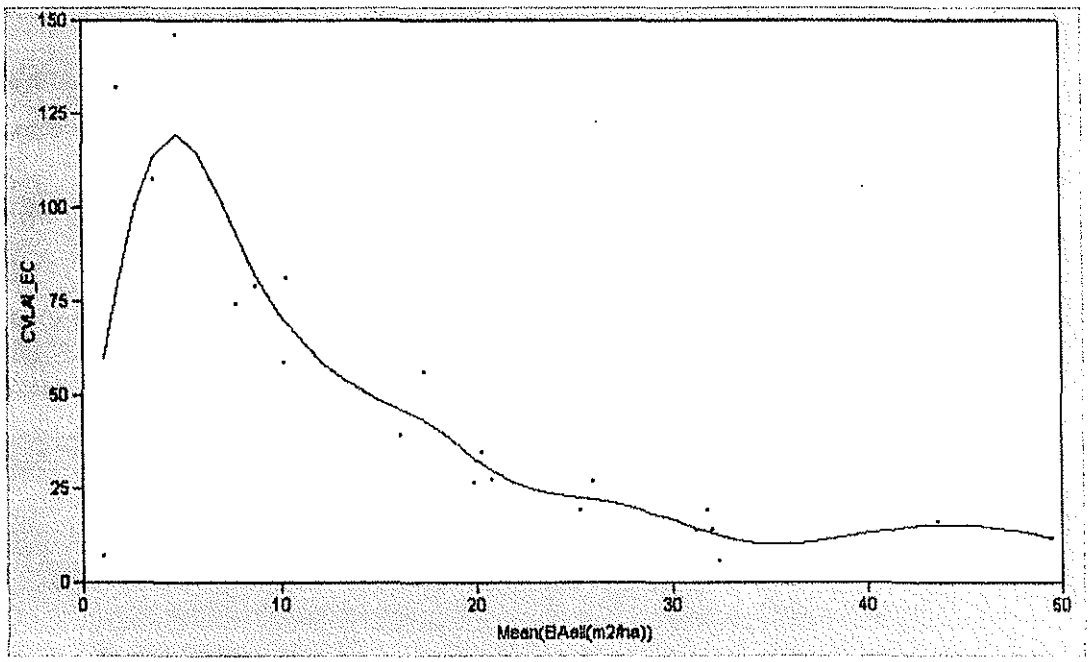

Figure 3.10 Basal Area is regressed against camera estimated LAI for four iterations of aggregation within the 40 m x 40 m plots. The coefficient of variation is shown for each regression, and the dashed lines on the plots reflect a confidence interval at $\alpha = 0.15$. All relationships are significant at $p<0.0001$

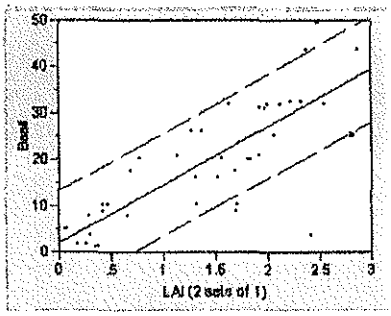

2 sets of 1
$R^2 = 0.62$

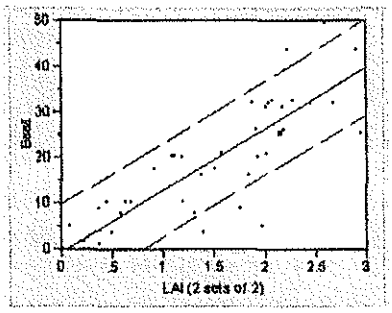

2 sets of 2
$R^2 = 0.68$

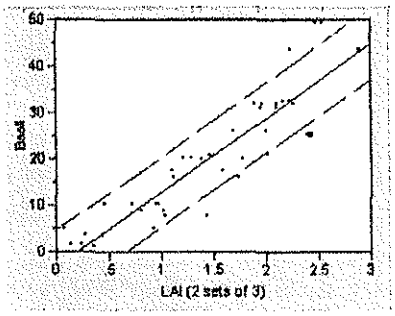

2 sets of 3
$R^2 = 0.83$

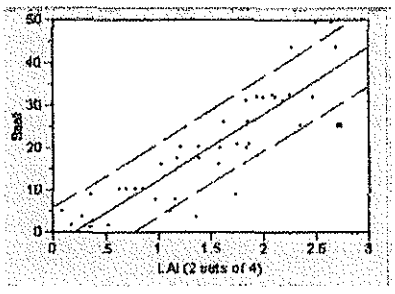

2 sets of 4
$R^2 = 0.77$

Chapter 4

Estimating Biophysical Parameters with Remotely Sensed AISA Imagery

Introduction

To address the initial question "What can remote sensing tell us about canopy structure?," we have utilized two tools that take different approaches to viewing the canopy: a "top-down" view with remotely sensed imagery and a "bottom-up" view with the hemispheric camera. Since LAI is the primary measure of canopy that this project has chosen to utilize, the final step becomes reconciling the estimated LAI values from the hemispheric camera system with the remotely sensed data in the form of vegetation indices. More specifically, it is necessary to determine whether there is a relationship between the remotely sensed data (AISA imagery) and the estimations of canopy cover (LAI, etc.). Such a relationship would allow for estimation of canopy cover through LAI for the entire area covered by the flight line of the AISA instrument.

While reconciling LAI estimates from the hemispheric camera with vegetation index estimates from the AISA sensor may seem straightforward, this is in fact a fairly complicated task due to differences in spatial resolution. The spatial resolution of the AISA sensor is explicit (3m spatial resolution), while the resolution of the camera is not. The resolution of the camera depends on the density of surrounding vegetation, with increasing tree cover reducing the effective spatial resolution. With the concentric ring system that the camera uses, the inner most rings, which correspond to the area directly above the camera, are more sensitive to LAI within them than each resulting outer ring. In other words, the presence of canopy within the inner rings is weighted more heavily

than the presence of canopy within the outer rings. Therefore, resolvable trees on the horizon of the image may be included in LAI estimation analysis, even if there is no actual tree cover above or within several meters of the camera system. So while the presence of canopy is more important in the inner rings, presence in the outer rings can still result in an LAI measure even if no canopy is present within several meters. As a result, determining the spatial extent and its effective resolution for comparison with spectral data is difficult.

In the third chapter, it was determined that taking 3 measurements about 10-15 m apart could effectively describe canopy density for a 40 m x 40 m area. For this portion of the study the index values from the AISA sensor are easily manipulated in regards to spatial resolution because the resolution is explicitly defined and undoubtedly smaller than the spatial coverage of the camera. The resolution of the AISA pixels is 3 meters, so that 1 pixel measures 3 m x 3 m. Therefore, single LAI estimates will still be used for comparison with the indices. First, single LAI estimates will be tested against single pixel index values, and then the resolution of the index values derived from the AISA reflectance spectra will be manipulated to determine the optimal spatial resolution for LAI estimation.

Prior to analysis of the data, it seems likely that three pixel aggregations of the AISA data would correspond most closely with tree data for two reasons: first, data collected in the 40 m x 40 m plots were collected in 10 m x 10 m subplots, where the scale is much more closely approximated by the 3 pixel (9 m x 9 m) average; second, the scale of individual trees is also more closely approximated by the 3 pixel average, where individual open-grown trees typically have canopy diameters between 8 and 10 m (Ding,

2002). However, because trees in open canopies are less stressed by competition (for light, in particular), these tree canopy diameters are certainly larger than those that would typify dense stands (Mitchell, et al., 1997).

Methods

Ground data was collected at the Bessey Unit of the Nebraska National Forest (BU/NNF) located near Halsey, Nebraska. The BU/NNF is a 25,000 ha unit, of which app. 10,000 ha contain trees. The forested areas contain predominantly ponderosa pine (*Pinus ponderosa)* and eastern red cedar (*Juniperus virginiana)*, which were planted in the early 1900s. Spectral imagery was collected with an AISA imaging spectrometer. The sensor gathers data at selectable wavelengths between 430 and 900 nm at a selectable spatial resolution. For this experiment, the spatial resolution was approximately 3m. The AISA data acquisition over the BU/NNF occurred on August 10, 2002. The resulting flightline covered a swath of the forest approximately 11 km long and 900 m wide, covering 990 ha (Figure 1.1). The area contains a wide range of canopy covers, from open grassland to savanna to closed canopy forest. A suite of 5 vegetation indices were calculated on the AISA data. A summary of how these indices were selected can be found in Chapter 2, and a list and description of the indices can be found in Table 1.1 and Appendix I, respectively.

Analysis of 40 m x 40 m plots

Direct measures of tree density (basal area, tree density, etc.) and estimated LAI data were measured in the 40 m x 40 m plots selected for study by previous UNL researchers. Each plot is divided into 16 – 10 m x 10 m subplots. These 8 plots included 4 plots that are medium to high density (4, 9, 10, and 11; average LAI = 2.18, 2.49, 2.30,

and 2.54 respectively, Ellipsoid-Campbell method) and 1 plot that is considered much more heterogeneous (16, average LAI = 1.17). Three additional plots were created in an attempt to improve the range of variability between plots. These plots (21, 22, and 23) included 1 plot that represents the most dense area within the flightline (21, average LAI = 2.58) and two plots that represent the least dense areas within the flightline (22 and 23; average LAI = 0.36 and 0.35, respectively). DOQQ images of these plots, the NDVI image, pixel distribution, and average LAI value can be seen in Figure 4.1. LAI measurements were taken in 8 of the 16 subplots, while DBH and pine litter biomass were measured in every subplot. Some subplots were not measured as a result of inaccessibility or oversight, which resulted in 59 total measurements. DBH was converted to basal area on a subplot basis.

Regressions between individual subplot LAI values for single points (using the Ellipsoid-Campbell logarithmic method) and the AISA vegetation index values were performed. Because the effective resolution of the camera is almost certainly larger than the 3 m x 3 m spatial resolution of the AISA sensor, the AISA pixels were aggregated to pixels measuring 9 m x 9 m (a 3 pixel x 3 pixel aggregation) and again compared to the LAI values through regression. Finally, a regression was performed between the LAI values averaged over the entire plot (all 8 subplots) and the index values for a 39 m x 39 m (13 pixel aggregation) area that approximated the size of a plot. Similar regressions were performed for the above iterations between direct measures of tree density, such as basal area and litter quantity, and the index values.

Analysis of 100 points

The relatively low variability in LAI within the eight 40 m x 40 m plots led to the creation of another sampling scheme designed to take advantage of the full range of cover types within the flight line. An unsupervised classification was performed on the full AISA image dataset, creating 20 classes. These classes were labeled as tree or non-tree based on a priori knowledge of the area within the flightline. Within the tree class, 67 points were randomly chosen throughout the entire image. Likewise, 33 points were randomly selected within the non-tree class. The result of these point selections was 100 points randomly chosen from the entire image area that presumably encompassed the entire gradient of canopy covers from open grassland to closed canopy forest. Of the points within the tree class, approximately 20 plots contained or were adjacent to one or more eastern red cedar trees. The area surrounding most of these plots is predominantly ponderosa pine with some eastern red cedar interspersed throughout the area presumably viewable by the LAI camera. Of these 20 plots, only 4 were located in pure cedar stands. After the points were selected, 96 of the points were visited and hemispheric images were taken for LAI estimation. One was not visited, and three of the points were inaccessible, leaving a total of 96 points. Of the 33 grassland points, 4 had trees close enough to the plot that LAI was detected with the hemispheric camera. The other 29 points were not close enough to trees for an LAI measurement to be taken. However, because these points were in grassland areas, they still show a wide variety of values for the various indices. NDVI values can be as high as 0.50 for these zero canopy LAI values because of the grassland species present.

The LAI estimates were first compared with the vegetation index values derived from the AISA data at the 1 pixel (3m x 3m) spatial resolution. LAI was regressed against the pixel value of each of the six vegetation indices for each of the 96 points randomly selected from the flightline. Because the LAI hemispheric camera system almost certainly has a spatial footprint greater than the 3 m area encompassed by an AISA pixel, the AISA data was aggregated to successively larger sizes until an area of approximately 40 m x 40 m was reached. The resulting values for each series of aggregations were regressed against the single estimated LAI value for that point.

Results and Discussion

Histograms showing the distribution of LAI in both the 100 points and the 40 m plots are shown in Figure 4.2. Both show a more or less bimodal distribution with modes centered around LAI values of approximately 0.25 and 2.5. While this may be expected within the 40 m plots because of their relative homogeneity, it is surprising that the 100 points, which were chosen specifically to span the cover gradient from zero cover to closed canopy forest, are similarly distributed. In the 40 m plots, there is a gap around an LAI value of 1. In the 100 points data, gaps also appear, though smaller and at different points (most notably at LAI between 0.75 and 1) along the LAI continuum. While these results indicate that our selection of points may not have done an adequate job of spanning the range of canopy cover at the NNF, it may also be a result of limitations of the LAI camera system. Because the inner rings are weighted greater than the outer rings in the analysis of the camera images for LAI, any trees that are beyond the immediate area probably contribute almost equally to the LAI detected. Essentially this constrains what the camera views. If the canopy doesn't reach into the inner-most rings, the

resulting LAI value is quite low. Some evidence of this can be seen in Figure 3.2, where the image with only two trees visible results in an LAI value of 0.21. LAI values around 1 are consequently difficult to obtain as there is either enough canopy to reach the inner rings and push the LAI value higher, or there are only trees on the periphery that result in fairly low values that are constrained between 0 and 0.5. It may be possible that these values of LAI around 1 are difficult to obtain simply because they are uncommon within the forest. Because the tree stands are even-aged stands (they were all planted at essentially the same time), it is possible that the size or configuration of trees that would produce an LAI estimation of 1 is simply not present within the BU/NNF. Values of LAI were also constrained on the upper end of the distribution (Figure 4.2). Individual measurements reached as high as 3.5, but at the plot scale (40 m x 40 m) the upper limit was approximately 3.

When LAI was regressed against the vegetation indices for the 100 points data on a single pixel basis, the NDVI showed the highest R^2, followed by the WDRVI (α=0.15 and α=.1) and the VARI (Figure 4.3). The R^2 values for these 4 regressions were somewhat similar (within .04 of each other), while the RRDI red edge and the GNDVI had the lowest coefficients of determination of the group. The results were similar for the 40 m plots at the 1 pixel scale, where NDVI had the highest coefficient of determination, followed by the WDRVI (α=0.15) (Figure 4.3). However, the RRDI red edge showed the next highest R^2, while the VARI and GNDVI showed the two lowest values. The RRDI utilizing the red edge was hypothesized to have the highest correlation with LAI because of its use of specific wavebands available on the AISA platform. At this spatial resolution, however, this is not the case, as the NDVI and WDRVI performed better in

both the 100 points and the 40 m plot dataset. From these datasets, the RRDI red edge and the GNDVI seem to be the least effective indices for correlating with LAI.

When the spatial resolution of the index data was aggregated to 3 pixels (9 m x 9m), the coefficients of determination improved slightly, as expected (Figure 4.3). In the 100 points data, VARI showed the highest R^2, followed by the NDVI and the WDRVI (α=0.15). The GNDVI and RRDI red edge coefficients of determination still remained the lowest. NDVI still showed the highest R^2 in the 40 m plot dataset with the 3 pixel aggregation. The RRDI red edge and WDRVI (α=0.15 and α=0.1) were the next highest, while the GNDVI and VARI had the lowest coefficients of determination. Interestingly, VARI had the highest coefficient of determination in the aggregated 100 points data, but the lowest in the 40 m x 40 m plots. Like the single pixel analysis above, the RRDI was not as effective as the NDVI in both the 100 points and 40 m x 40 m datasets. The VARI and WDRVI both performed better than the RRDI in the 100 points dataset, as well. These results indicate that the RRDI using the red edge is not as effective as the NDVI-based indices for correlating spectral data with LAI. While the coefficient of determination of the WDRVI is not as high as the NDVI, it is increasing the linearity of the NDVI/LAI relationship, where NDVI begins to lose sensitivity at higher LAI values. The WDRVI has a more linear relationship than NDVI. This is more apparent in the 100 points data, though both the RRDI and VARI indices also show a fairly linear response.

The 40 m x 40 m whole plot averages (where AISA data was averaged over the approximate plot area with a 13 pixel x 13 pixel average from the center point) showed a linear response between estimated LAI and all of the variables of interest (basal area and vegetation indices) (Figure 4.4). All of the indices had coefficients of determination

between 0.92 and 0.94 (Figure 4.4). The basal area/ LAI regression showed an R^2 of 0.86. While the sample size for these regressions is small (n=8), the results provide some indication of the scale at which the variables of interest and/or estimated LAI can be used to predict the other variable with high confidence. While the whole plots are larger than a Landsat pixel, these results indicate that at scales approximating (or exceeding) that of a Landsat pixel, all of these indices are very effective at estimating LAI.

A regression was also performed using the index values and basal area at three general scales within the 40 m x 40 m plots: the single pixel (3 m x 3 m) scale, the subplot scale (10 m x 10 m), and the whole plot scale (40 m x 40 m). At the single pixel (3m) scale, the RRDI Red Edge index showed the highest coefficient of determination, though the NDVI, WDRVI (α=0.1 and α=0.15), and VARI all had coefficients of determination within 0.03 of the RRDI Red Edge (Table 4.1). The GNDVI had the lowest coefficient of determination. At the 3 pixel (9m) resolution (approximating the subplot scale), VARI, RRDI red edge, and the WDRVIs (α=0.1 and α=0.15) all had coefficients of determination that were within 0.003 of 0.6 (Table 4.1). The NDVI was also quite similar, with an R^2 of 0.581. The GNDVI again had the lowest R^2 of the group. At the plot scale (13 pixel, 39 m, approximating the 40 m plot scale), all indices showed an R^2 above 0.84 (Table 4.1). The VARI had the highest R^2 (0.9), followed by the RRDI, the WDRVIs, NDVI, and GNDVI, respectively.

The 100 points data allowed for an analysis of how the relationship between the indices and LAI changes with increased spatial resolution. As the AISA data indices were aggregated to larger and larger pixel sizes, the trend in R^2 was to increase up to the 9 pixel (27 m x 27 m) aggregation, at which point all the indices declined (Figure 4.5).

However, two of the indices (NDVI and GNDVI) peaked at the 7 pixel (15 m x 15 m) resolution. NDVI had the highest initial R^2 at the 1 pixel (3 m x 3 m) resolution, but VARI had the highest R^2 at each of the successive resolutions (Figure 4.5). This data supports the basal area results which indicate the best relationships between indices and variables of interest occur at scales approaching the resolution of a 30 m Landsat TM pixel. At the 7 pixel (21 m x 21 m) aggregated resolution, the coefficients of determination are the highest for all but the two WDRVIs, and aggregation to 9 pixels (27m x 27 m) does not increase the coefficient of determination significantly.

Conclusion

At the BU/NNF, because trees typically occur in even-aged stands, there is a lack of areas where LAI is approximately 1. Limitations of the camera system may also contribute to the lack of estimated LAI values in this range. More research is necessary to determine exactly why there are few LAI values of approximately 1, as it could be either of the reasons mentioned above. The upper limit of LAI values at the BU/NNF was observed between 3 and 3.5, which is coincident with the hypothetical limit of 3 stated by Law et al (2002).

Generally, NDVI and VARI were more highly correlated with the camera LAI estimates than any of the other indices. With the exception of the 40 m x 40 m plot results, where VARI performed the worst of the indices, these two indices showed the highest coefficients of determination for a majority of the regressions performed. The RRDI, which was hypothesized to perform the best of these indices because it makes use of very specific wavebands that are not commonly available on commercial satellite

sensors (Landsat TM and MODIS, for example), was not as effective as the VARI and NDVI indices, which can be calculated by most remote sensing platforms.

This experiment indicates that the high spatial resolution of the AISA sensor is more useful than the high spectral resolution when the relationship between spectral data and LAI is considered. While the best relationships between LAI and vegetation indices occur at scales between 15 and 30 m, the relationships at higher spatial resolutions are as good or better than many published values (Gong, et al., 1995; Lee, et al., 2004; Nemani, et al., 1993; Schlerf, et al., 2005).

It is difficult to endorse a single index for estimating LAI in ponderosa pine from remotely sensed data. The VARI outperformed NDVI as a correlate with LAI in the 100 points data, but NDVI was the more effective index in most of the other analyses. VARI, which was designed as more of a chlorophyll estimation index, performs surprisingly well compared to NDVI. Its use of only visible channels also makes it an intriguing index for further study as few studies have examined the relationship between VARI and LAI.

Figure 4.1 DOQ subset images are shown at left of (from top) plots 22, 16, and 21. In the DOQ images, trees appear as dark portions of the image. NDVI subsets of the plots are shown at right, along with the distribution of NDVI pixels below the plot cutouts (pixels are at 3 m resolution). In the NDVI images, lighter shades indicate higher NDVI values. Average LAI estimates for the whole plot are also shown.

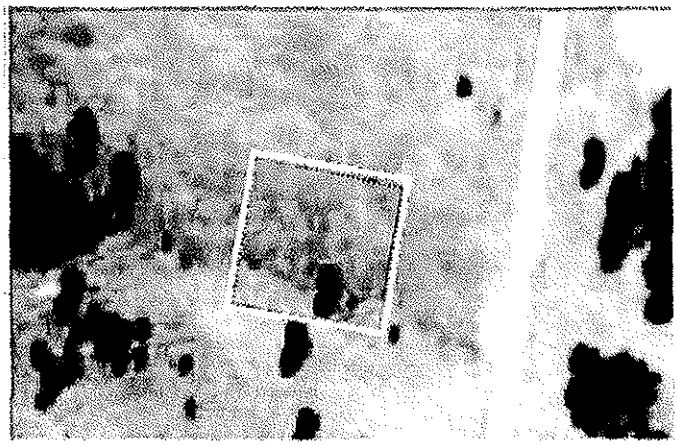

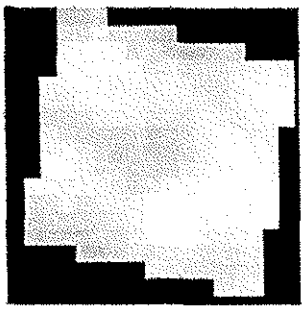

Avg. LAI = 0.36

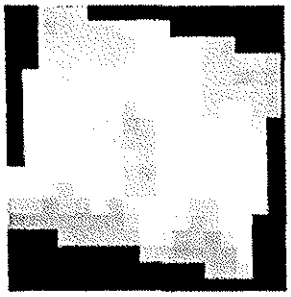

Avg. LAI = 1.17

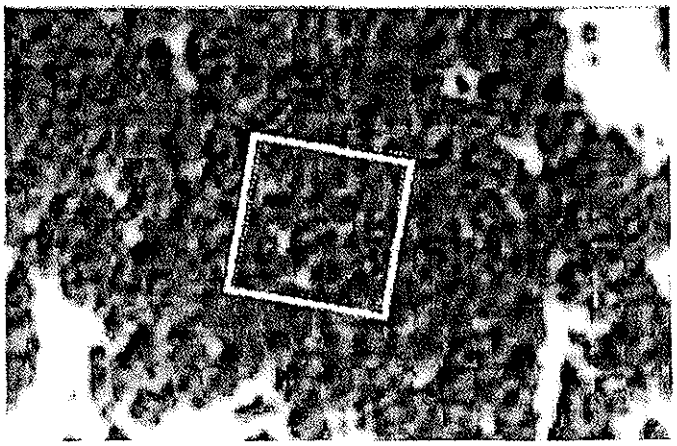

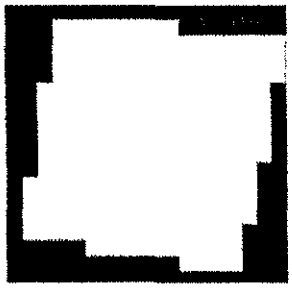

Avg. LAI = 2.59

Figure 4.2 Histogram distributions of LAI are shown for both the 40 m x 40 m plot (left) and the 100 points (right) datasets.

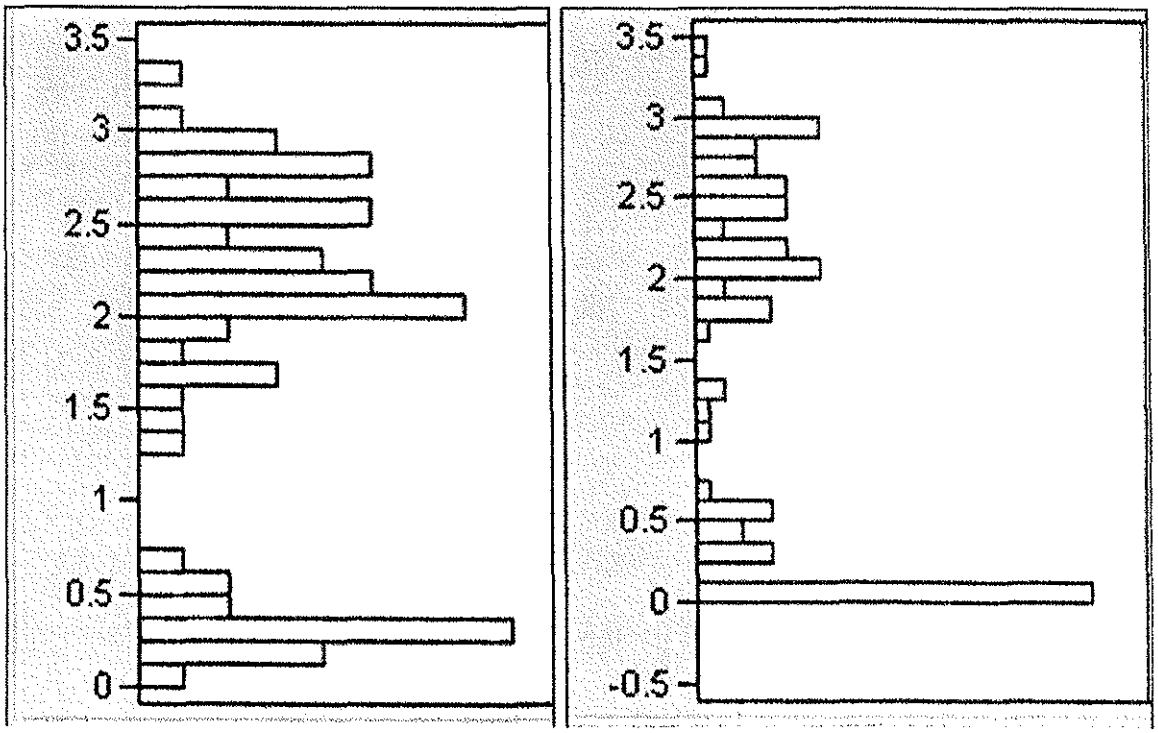

Figure 4.3 LAI (x-axis) is plotted against 4 of the vegetation indices for 100 points data. The coefficient of determination (R2) is displayed on each plot. The summarized R2 data is shown in the chart below the plots for both the 100 points dataset and the 40 m x 40 m dataset at two resolutions (1 pixel (3m) and 3 pixel (9 m)). All relationships are significant at $p < 0.001$

NDVI →

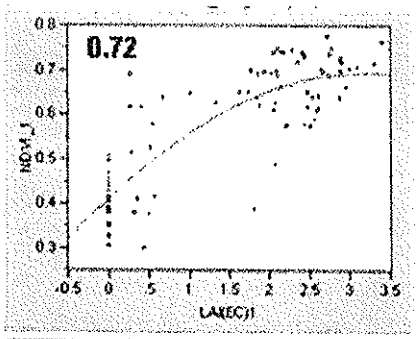

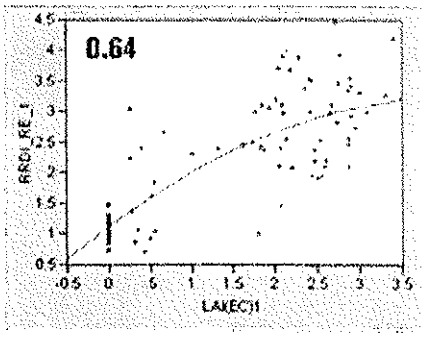

← RRDI

VARI →

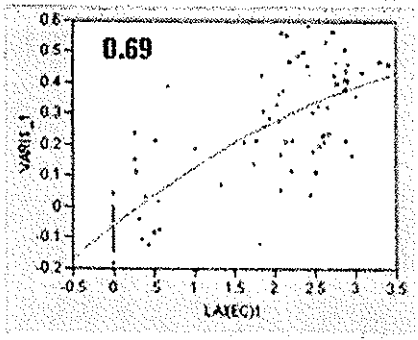

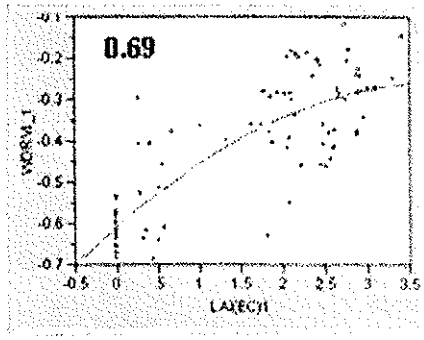

← WDRVI (α=0.01)

Index	100 Points	100 Points	40m x 40m plots	40 m x 40 m plots
	R^2 - 1 pixel (3m x 3m)	R^2 - 3 pixel (9 m x 9m)	R^2 - 1 pixel (3 m x 3m)	R^2 - 3 pixel (9 m x 9m)
NDVI	0.718	0.771	0.612	0.731
RRDI_RE	0.641	0.703	0.576	0.71
VARI	0.688	0.786	0.49	0.642
WDRVI (.05)	0.678	0.749	0.556	0.691
WDRVI (.1)	0.691	0.734	0.588	0.701
WDRVI (.15)	0.699	0.756	0.577	0.708
GNDVI	0.636	0.69	0.547	0.687
	n=93	n=93	n=59	n=59

Figure 4.4 40 m x 40 m plot averages regressing basal area and three of the indices (Y) vs. LAI (X). The R^2 is shown in the center table for each of these comparisons. All relationships are significant at $p < 0.001$.

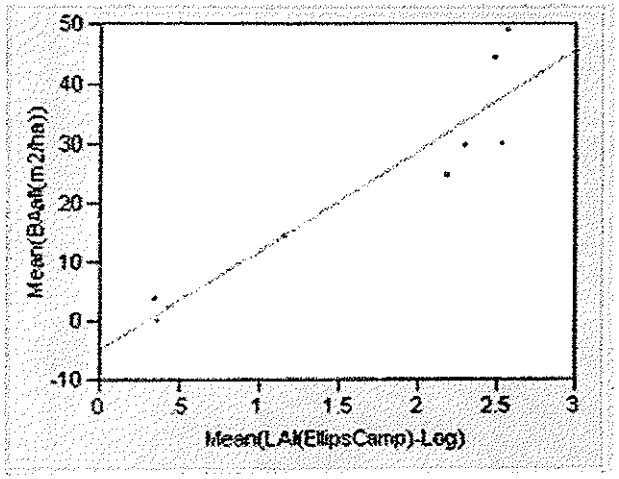

Variable	R^2
Basal Area	0.862
GNDVI	0.921
NDVI	0.922
RRDI_RE	0.938
VARI	0.925
WDRVI_05	0.928
WDRVI_1	0.929
WDRVI_15	0.928

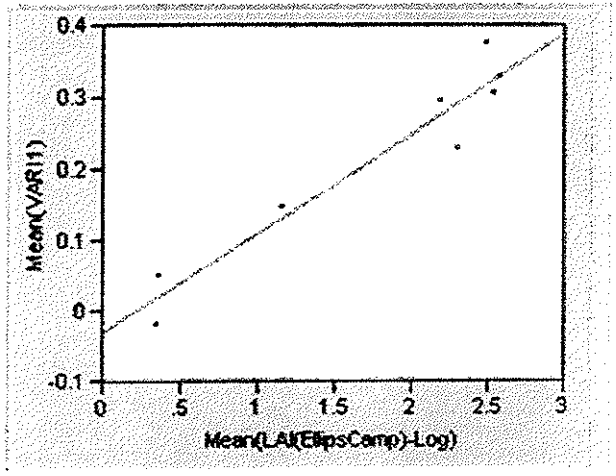

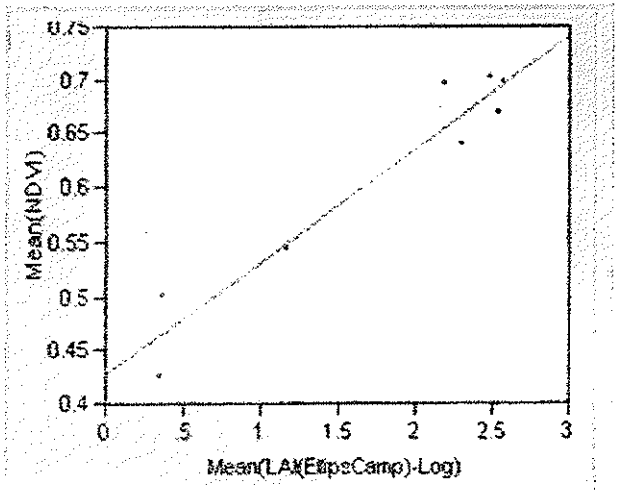

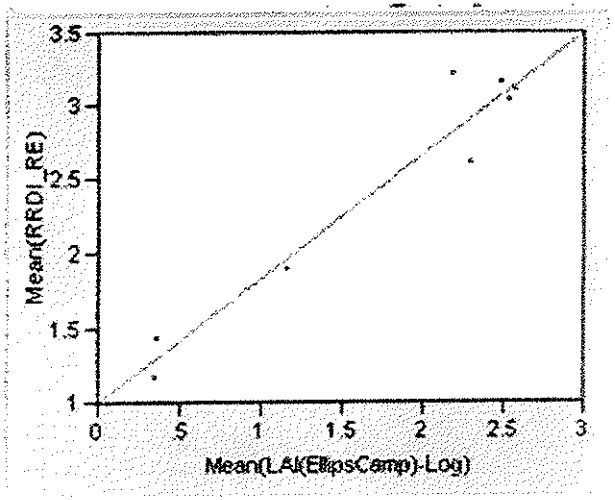

Figure 4.5 100 points data showing how the coefficient of determination (R^2) changes with decreasing spatial resolution. All relationships are significant at $p < 0.001$

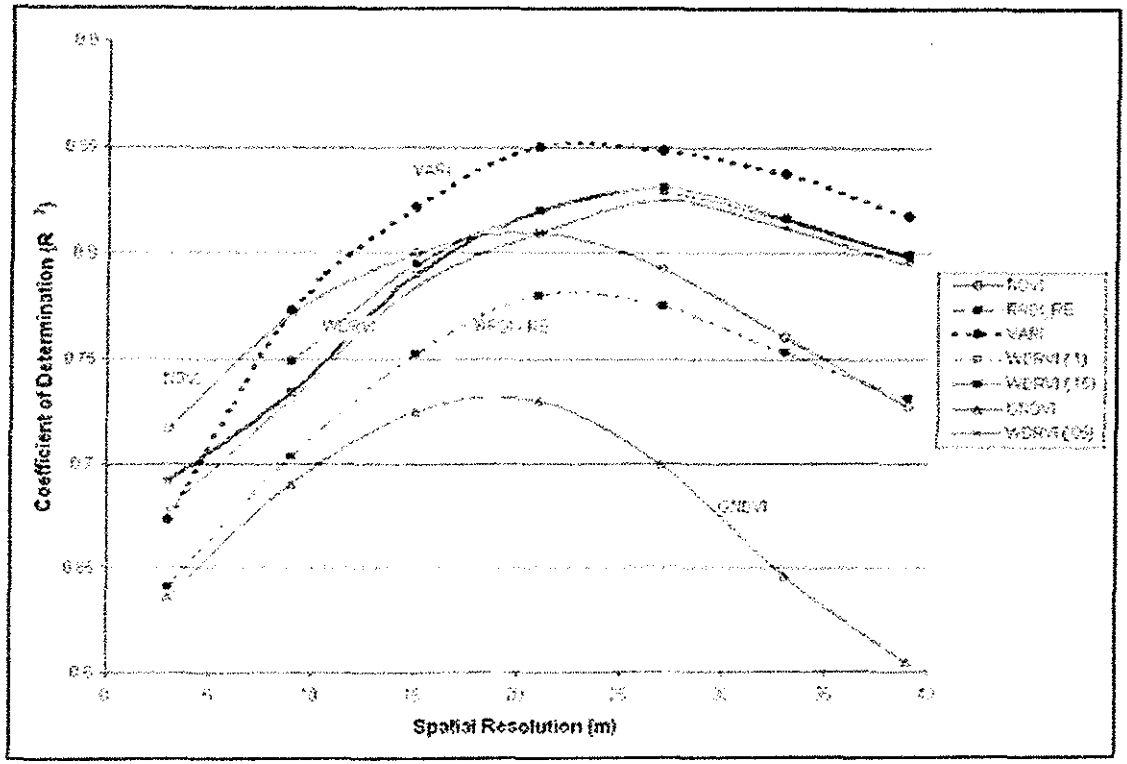

	R^2 - 1 pixel (3 m x 3 m)	R^2 - 3 pixel (9 m x 9 m)	R^2 - 5 pixel (15 m x 15 m)	R^2 - 7 pixel (21 m x 21 m)	R^2 - 9 pixel (27 m x 27 m)	R^2 - 11 pixel (33 m x 33 m)	R^2 - 13 pixel (39 m x 39 m)
NDVI	0.397	0.499	0.585	0.81	0.593	0.539	0.486
RRDI_RE	0.332	0.418	0.509	0.78	0.551	0.514	0.477
VARI	0.392	0.547	0.65	0.85	0.698	0.669	0.626
WDRVI (.05)	0.371	0.463	0.532	0.81	0.6	0.571	0.539
WDRVI (.1)	0.379	0.456	0.54	0.82	0.606	0.577	0.546
WDRVI (.15)		0.466	0.545	0.82	0.61	0.58	0.543
GNDVI	0.293	0.348	0.452	0.73	0.452	0.393	0.348

Table 4.1 Results of indices regressed against basal area at three spatial resolutions in the 40 m x 40 m plots - results in table are coefficients of determination (R^2) for 2nd order polynomial fits. Relationships are significant at $p < 0.001$ unless otherwise noted.

	Spatial Res.	Index					
Variable		GNDVI	NDVI	RRDI - RE	VARI	WDRVI (.1)	WDRVI (.15)
Basal Area	3 m	0.467	0.533	0.557	0.533	0.547	0.546
Basal Area	9 m	0.539	0.581	0.601	0.6	0.598	0.597
Basal Area	39 m	0.847[2]	0.857[2]	0.876[2]	0.9[1]	0.874[2]	0.872[2]
1 - significant at p < 0.01							
2 - significant at p < 0.005							

Chapter 5

CONCLUSION

The original question that provided motivation for this thesis asks "What can remotely sensed imagery tell us about ponderosa pine canopy structure?" Such a question is purposely vague, and leads to other questions. For example, the question "what is canopy structure?" is a legitimate one. Canopy structure can be defined in more than one way. There are both vertical and horizontal aspects to canopy structure. The horizontal aspect of canopy structure involves how tree canopies are distributed as a result of a tree's spatial relationship with other trees around it. The vertical aspect of canopy structure involves how trees distribute canopy throughout the vertical profile. These aspects of canopy structure do not act independently of each other. Vertical distribution of canopy is affected by the proximity of other trees.

For this project, estimates of vertical structure took the form of LAI estimations. This is a commonly used measure of leaf distribution throughout a canopy, but as was stated in chapter 3, it is a far from perfect measure. One of the difficulties in measuring canopies is that there is no true measure of canopy structure. LAI, which attempts to characterize structure in terms of leaf area over a given ground area, is not a complex concept by definition, but in practice is difficult to measure. Organization (nonrandomness) at different levels within canopies, instrument limitations, and woody (non-photosynthesizing) vegetation can confound estimation of LAI. The results of chapter 3 showed that to adequately characterize the variability in LAI of the 40 m x 40 m plots, three measurements approximately 15 m apart need to be taken. Also, within this project, the measures of LAI were actually plant area index (PAI), which includes

non-photosynthetic vegetation. The extent to which this affected the measurements of LAI is unknown. Law et al. (2002) suggests woody vegetation can inflate LAI values 10-30%). Nevertheless, the LAI measures observed fell within the range of LAI values commonly observed in ponderosa pine. The camera system may provide some tools to correct for this woody vegetation fraction with its classification scheme that allows different objects within the canopy image to be differentiated based on color. The viability of this method has not been tested, however.

The camera system provides a more useful estimation of LAI than the ceptometer system, as was shown in chapter 3. While the camera has limitations, it provided a useful tool for estimating LAI in ponderosa pine woodlands. It also has capabilities beyond what it was used for in this experiment. The software can model diurnal and seasonal variation in the light environment at the point of image acquisition. For some applications, this may be more important than canopy characterization, where branch or needle interception may not be important. In other words, the "canopy" itself may not be as important as what the impact of the canopy is on a given point or area. For these types of applications, the camera may be effective with a single point measurement.

The results from chapter 2 provided insight into the behavior of the vegetation indices selected for this project. While EVI and SAVI were excluded from the analysis as a result of the analyses in chapter 2, they raised some interesting questions about the influence of nonphotosynthetic background materials. The results from chapter 2 indicate that background may contribute significantly to the grassland signal, in contrast to its role in the forested areas. The shadowing effect of the trees may interact with the strength of the background signal.

The seasonal variation in index values also is brought into question in chapter 2. Clearly, high index values (NDVI, particularly) are not restricted to forested areas, but there seems to be a constraint on the NDVI values in grassland areas as a result of water availability. This constraint is absent in the wet meadows of the Barta Brothers Ranch when water is readily available for plant uptake. Contrasts between seasonal index curves at the BU/NNF and the Barta Brothers Ranch could offer some useful insights about the temporal variability in vegetation response within the Nebraska Sand Hills region.

In trying to study canopy structure, the horizontal or spatial configuration of trees was addressed, though other possibilities exist for further study. One possibility for developing a better understanding of the spatial configuration of trees is to employ landscape metrics to describe canopy pattern. Landscape metrics provide quantitative analyses of pattern in landscapes. Examples that could be useful for describing spatial configuration include patch size, patch connectivity and perimeter-to-area ratio. Once an index has been selected for its ability to distinguish tree from non-tree (see chapter 2), landscape metrics can easily be performed on the dataset. When used with the AISA data, the increased spatial resolution may provide useful information that is not available with other, lower resolution sensors. Of particular interest may be the differences that occur between the area burned in 1965 and the remaining unburned area, or the differences between ponderosa pine canopy cover and eastern red cedar canopy cover. Metrics that measure patch size or distribution along with good ground data may provide information about potential fire risk or why animal species are found in certain areas. Presently, research has begun at the BU/NNF on the American Burying Beetle

(*Nicrophorus americanus*), an endangered species that is found at the BU/NNF. Landscape metrics may be useful for answering why this species is found at certain places and not others. The application of landscape metrics could be useful in helping to answer many research questions at the BU/NNF.

Chapter 4 provided insights into the relationship between vegetation indices and estimated LAI. The VARI and NDVI proved to be the most useful indices for correlating spectral data with LAI. At a spatial resolution of 15 m, the LAI and index data showed strong relationships that meet or exceed published relationships of the same type. While the narrow band spectral data available with the AISA sensor did not prove to be as advantageous as originally hypothesized, it is possible that the indices used and tools chosen to analyze the spectral data did not fully take advantage of the AISA capabilities. The 1st principle component image showed some promise with respect to separating tree and non-tree cover types, and though a standardized index was not developed, the possibility to do so is still present.

The AISA sensor, with its high spatial and spectral resolution capabilities, can be a powerful tool if proper care is given to the questions being asked. Specific goals and clear questions are needed to fully utilize the capabilities of AISA sensor system. In this project, very little evidence was found to support the use of a hyperspectral system over any other system that is capable of calculating the most common indices (NDVI, VARI, WDRVI) at a high spatial resolution. Hyperspectral data are useful for a variety of applications, such as classification of cover that show small spectral differences (pine/cedar separation, for example), estimation of pigment concentrations that require

very specific wavelengths, and studies that need near-continuous spectral coverage through the visible and near-infrared portions of the spectrum.

References

Agee, J. K. 1998. Ecology and biogeography of *Pinus*: an introduction. In Ecology and Biogeography of *Pinus*, ed. David M. Richardson, pp 3-40, Cambridge, United Kingdom: Cambridge University Press

Archer, Steve. 1990. Development and stability of grass/woody mosaics in a subtropical savanna parkland, Texas, U.S.A. Journal of Biogeography 17: 453-462

Alexander, R. A. 1986. Silvicultural Systems and Cutting Methods for Ponderosa Pine Forests in the Front Range of the Central Rocky Mountains. USDA Forest Service General Technical Report RM-128. 22 p. Rocky Mountain Forest and Range Experiment Station, Fort Collins, CO.

Asner, G. P., Wessman, C. A., and Schimel, D. S. 1998. Heterogeneity of Savanna Canopy Structure and Function from Imaging Spectrometry and Inverse Modeling. Ecological Applications 8 (4): 1022-1036

Baret, F., and Guyot, G. 1991. Potentials and Limits of Vegetation Indices for LAI and APAR Assessment. Remote Sens. Environ. 35: 161-173

Bonan, G. 1993. Importance of leaf area index and forest type when estimating photosynthesis in boreal forests. Remote Sens. Environ. 43: 303-314

Bonan, G. B. 1995. Land-atmosphere interactions for climate system models: coupling biophysical, biogeochemical, and ecosystem dynamical processes. Remote Sens. Environ. 51: 57-73

Boyd, D. S., Wicks, T. E., and Curran, P. J. (2000). Use of middle infrared radiation to estimate the leaf area index of a boreal forest. Tree Physiology 20: 755-760

Campbell, G. S. 1986. Extinction Coefficients for Radiation in Plant Canopies Calculated Using an Ellipsoidal Inclination Angle Distribution. Agric. For. Meteorol. 36: 317-321

Chen, J. M., and Cihlar, J. (1996) Retrieving leaf area index of boreal conifer forests using Landsat TM images. Remote Sens. Environ. 55: 153-162

Covington, W.W. and Moore, M. M. 1994. Southwestern ponderosa forest structure: changes since Euro-American settlement. Journal of Forestry 92:39-47

Covington, W. W., Fulé, P. Z., Moore, M. M., Hart, S. C., Kolb, T. E., Mast, J. N., Sackett, S. S., and M. R. Wagner. 1997. Resotring Ecosystem Health in Ponderosa Pine Foresets of the Southwest. Journal of Forestry, April 1997, pp. 23-29

Ding, X. 2002. Effects of Ponderosa Pine Forest Establishment on Nitrogen Cycling in the Nebraska Sandhills. Master's Thesis, Natural Resource Sciences, University of Nebraska – Lincoln

Emly, V., Sprentall, R., Lachowski, H., Varner, V., and Maus, P. 1997. Integrating remote sensing into classification of ecological habitat types and seral stages. ACSM/ASPRS Annual Convention & Exposition Technical Papers. Vol. 4: 600-609

Fassnacht, K. S., Gower, S. T., MacKenzie, M. D., Nordheim, E. V., and Lillesand, T. M. (1997). Estimating the leaf area index of north central Wisconsin forests using the Landsat thematic mapper. Remote Sens. Environ. 61: 229-245

Fernandes, R., Miller, J. R., Hu, B., and Rubinstein, I. G. (2002). A multiscale approach to mapping effective leaf area index in boreal *Picea marina* stands using high

spatial resolution CASI imagery. International Journal of Remote Sensing 23: 3547-3568

Fulé, P. Z., Covington, W. W., and Moore, M. M. 1997. Determining Reference Conditions for Ecosystem Management of Southwestern Ponderosa Pine Forests. Ecological Applications 7 (3): 895-908

Galvao, L. S., Vitorello, I., and Pizarro, M. A. 2000. An adequate band positioning to enhance NDVI contrasts among green vegetation, senescent biomass, and tropical soils. International Journal of Remote Sensing 21 (9): 1953-1960

Gitelson, A. A., Kaufman, Y. J., and Merzlyak, M. N. 1996. Use of green channel in remote sensing of global vegetation from EOS-MODIS. Remote Sens. Envir. 58: 289-298

Gitelson, A. A., Kaufman, Y. J., Stark, R., and Rundquist, D. 2002. Novel algorithms for remote estimation of vegetation fraction. Remote Sens. Envir. 80: 76-87

Gitelson, A. A. 2003. Wide Dynamic Range Vegetation Index for Remote Quantification of Biophysical Characteristics of Vegetation. Journal of Plant Physiology 161 (2): 165-173

Gitelson, Anatoly A., Gritz, Yuri, and Merzlyak, Mark N. 2003. Relationships between leaf chlorophyll content and spectral reflectance and algorithms for non-destructive chlorophyll assessment in higher plant leaves. J. Plant Physiol. 160 (3): 271-282

Gong, P., Pu, R., and Miller, J. R. 1995. Coniferous Forest Leaf Area Index Estimation along the Oregon Transect Using Compact Airborne Spectrographic Imager Data. Photogrammetric Engineering & Remote Sensing 61 (9): 1107-1117

Goser, S. T., Hayes, B.E., Fassnacht, K. S., Running, S.W., and Hunt, E.R. Jr. 1993. Influence of fertilization on the allometric relations of two pines in contrasting environments. Can. J. For. Res. 23:1704-1711.

Gower, S. T., and Norman, J. M. 1991. Rapid Estimation of Leaf Area Index in Conifer and Broad-Leaf Plantations. Ecology 72 (5): 1896-1900

Gower, S. T., Kucharik, C. J., and J. M. Norman. 1999. Direct and Indirect Estimation of Leaf Area Index, f_{APAR}, and Net Primary Production of Terrestrial Ecosystems. Remote Sens. Environ. 70:29-51

Homyack, J. A., Harrison, D. J., and Krohn, W. B. 2005. Long-term effects of precommercial thinning on small mammals in northern Maine. Forest Ecology and Management 205 (1-3): 43-57

Henzlik, R. E. 1965. Biogeographic Extensions into a Coniferous Forest Plantation in the Nebraska Sandhills. American Midland Naturalist 74 (1): 87-94

Hu, B., Inannen, K., and Miller, J. R. (2000). Retrieval of leaf area index and canopy closure from CASI data over the BOREAS flux tower sites. Remote Sens. Environ. 74: 255-274

Hunt, J. C. 1965. The Forest that Men Made. American Forests – The Magazine of Forests, Soil, Water, Wildlife, and Outdoor Recreation. Nov. and Dec., 1965.

Huete, A. R. 1988. A soil adjusted vegetation index (SAVI). Remote Sens. Environ. 25: 295-309

Huete, A. R., Liu, H. Q., Batchily, K., and W. vanLeeuwen. 1997. A comparison of vegetation indices over a global set of TM images for EOS-MODIS. Remote Sens. Environ. 59 (3): 440-451

Kauffman, Y. J., and Tanre, D. 1992. Atmospherically resistant regetation index (ARVI) for EOS-MODIS. IEEE Transactions on Geoscience and Remote Sensing 30: 261-270

Keeley, J. E., and Zedler, P. H. 1998. Ecology and biogeography of *Pinus*: an introduction. In Ecology and Biogeography of *Pinus*, ed. David M. Richardson, pp 3-40, Cambridge, United Kingdom: Cambridge University Press

Koutsias, N., and Karteris, M. 2003. Classification analyses of vegetation for delineating forest fire fuel complexes in a Mediterranean test site using satellite remote sensing and GIS. Int. J. Remote Sensing 24 (15): 3093-3104

Law, B. E., Van Tuyl, S., Cescatti, A., and Baldocchi, D. D. 2001. Estimation of leaf area index in open-canopy ponderosa pine forests at different successional stages and management regimes in Oregon. Agricultural and Forest Meteorology 108: 1-14

Lee, K.-S., Cohen, W. B., Kennedy, R. E., Maiersperger, T. K., and Gower, S. T. 2004. Hyperspectral versus multispectral data for estimating leaf area index in four different biomes. Remote Sens. Environ. 91: 508-520

Little, S. N., and Shainsky, L. J. 1995. Biomass and nutrient distributions in central Oregon second-growth ponderosa pine ecosystems. Res. Pap. PNW-RO-481. Portland OR; USDA, Forest Service.

Marshall, J. D., and Monserud, R. A. 2003. Vertical trends in specific leaf area of three conifer species. Can. J. For. Res. 33: 164-170

Matrai, K., Szemethy, L., Toth, P., Katona, K., and Szekely, J. 2004. Resource use by red deer in lowland nonnative forests, Hungary. Journal of Wildlife Management 68 (4): 879-888

McPherson, G. 1997. Ecology and Management of North American Savannas. Tuscon: University of Arizona Press.

Mitchell, J. E., and Popovich, S. J. 1997. Effectiveness of basal area for estimating canopy cover of ponderosa pine. Forest Ecology and Management: 45-51

Nemani, R., Pierce, L., Running, S. and Band, L. 1993. Forest ecosystem processes at the watershed scale: sensitivity to remotely-sensed Leaf Area Index estimates. Int. J. Remote Sensing 14 (13): 2519-2534

Oker-Blom, P., and Smolander, H. 1988. The Ratio of Silhouette Area to Total Needle Area in Scots Pine. Forest Science 34 (4): 894-906

Peet, R. K. 1988. Forests of the Rocky Mountains, Pages 63-102 in M.G. Barbour and W.D. Billings (eds.) North American Terrestrial Vegetation. Cambridge University Press.

Peterson, D. L., Spanner, M. A., Running, S. W., and Teuber, K. B. 1987. Relationship of Thematic Mapper simulator data to leaf area index of temperate coniferous forest. Remote Sens. Environ. 22: 323-341

Price, J. C., and Bausch, W. C. 1995. Leaf Area Index Estimation from Visible and Near-Infrared Reflectance Data. Remote Sens. Environ. 52: 55-65

Ransome, D. B., Lindgren, P. M. F., Sullivan, D. S., and Sullivan, T. P. 2004. Long-term responses of ecosystem components to stand thinning in young lodgepole

pine forests. I. Population dynamics of northern flying squirrels and red squirrels. Forest Ecology and Management 202 (1-3): 355-367

Richardson, D. M., and Rundel, P. W. 1998. Ecology and biogeography of *Pinus*: an introduction. In Ecology and Biogeography of *Pinus*, ed. David M. Richardson, pp 3-40, Cambridge, United Kingdom: Cambridge University Press

Rouse, J. W., Haas, R. H. Jr., Schell, J. A., Deering, D. W. 1974. Monitoring vegetation systems in the Great Plains with ERTS. NASA SP-351, Third ERTS-1 Symposium NASA Washington DC. Vol. 1 pp 309-317

Rundel, P. W. and Yoder, B. J. 1998. Ecology and biogeography of *Pinus*: an introduction. In Ecology and Biogeography of *Pinus*, ed. David M. Richardson, pp 3-40, Cambridge, United Kingdom: Cambridge University Press

Running, S. W. 1990. A bottom-up evolution of terrestrial ecosystem modeling theory, and ideas toward global vegetation modeling. In *Modeling the Earth System,* UCAR/Office for Interdisciplinary Earth Studies, Boulder, CO 263-280

Running, S., and Gower, S. 1991. FOREST-BGC, a general model of forest ecosystem processes for regional applications: II. Dynamic carbon allocation and nitrogen budgets. Tree Physiology 9: 147-160.

Schlerf, M., Atzberger, C., and Hill, J. 2005. Remote sensing of forest biophysical variables using HyMap imaging spectrometer data. Remote Sens. Environ. 95: 177-194

Scholes, R. J., and Archer, S. R. 1997. Tree-Grass Interactions in Savannas. Annual Review of Ecology and Systematics 28: 517-544

Spanner, M. A., Pierce, L. L., Peterson, D. L., and Running, S. W. 1990. Remote sensing of temperate coniferous forest leaf area index: The influence of canopy closure, understory vegetation and background reflectance. Int. J. Remote Sensing 11 (1): 95-111

Stenberg, P. 1996. Correcting LAI-2000 estimates for the clumping of needles in shoots of conifers. Agric. For. Meteorol. 79: 1-8

Thill, R. E., and Koerth, N. E. 2005. Breeding birds of even- and uneven- aged pine forests of eastern Texas. Southeastern Naturalist 4 (1): 153-176

Turner, D. P., Cohen, W. B., Kennedy, R. E., Fassnacht, K. S., and Briggs, J. M. 1999. Relationships between Leaf Area Index and Landsat TM Spectral Vegetation Indices across Three Temperate Zone Sites. Remote Sens. Environ. 70: 52-68

Van Gardingen, P. R., Jackson, G. E., Hernandez-Daumas, S., Russell, G., and Sharp, L. 1999 Leaf area index estimates obtained for clumped canopies using hemispherical photography. Agric. For. Meteorol. 94: 243-257

Walter, J.-M.N., and Himmler, G. C. 1996. Spatial heterogeneity of a Scots pine canopy: an assessment by hemispherical photographs. Can. J. For. Res. 26: 1610-1619

White, J. D., Running, S. W., Nemani, R., Keane, R. E., Ryan, K.C. Measurement and remote sensing of LAI in Rocky Mountain montane ecosystems. Canadian Journal of Forest Research – Revue Canadienne De Recherche Forestiere 27 (11): 1714-1727.

WinSCANOPY 2002A, B For Canopy Analysis. 2002. Technical Manual. Copyright Régent Instruments, Inc. 2002

Wu, Y., and A. H. Strahler. 1994. Remote Estimation of Crown Size, Stand Density, and Biomass on the Oregon Transect. Ecological Applications Vol. 4, Issue 2: 299-312

Wylie, B. K., DeJong, D. D., and Tieszen, L. L. 1996. Grassland Canopy Parameters and their Relationships to Remotely Sensed Vegetation Indices in the Nebraska Sand Hills. Geocarto International Vol. 11 (3): 39-52

Wylie, B. K., Meyer, D. J., Choate, M. J., Vierling, L. V., and Kozak, P. K. 2000. Mapping woody vegetation and eastern red cedar in the Nebraska Sand Hills using AVIRIS. AVIRIS Earth Science & Applications Workshop Proceedings

Appendix I

Summary of Vegetation Indices

NDVI

The Normalized Difference Vegetation Index (NDVI) (Rouse, et al., 1974) is the most widely used index for studies utilizing remotely sensed data for assessment and monitoring of biophysical properties such as Leaf Area Index (LAI), vegetation fraction, fraction of photosynthetically absorbed radiation (fPAR), and net primary production. The equation for NDVI is as follows:

$NDVI = (\rho_{NIR}-\rho_R)/(\rho_{NIR} + \rho_R)$

The NDVI relies on the spectral contrast between the strong absorption in the red range (app. 670 nm) of the electromagnetic spectrum and the strong reflectance in the near-infrared range (above 700 nm) of the spectrum that characterizes green vegetation (Gitelson, 2003).

EVI

Originally designed for the MODIS satellite system, the Enhanced Vegetation Index, or EVI (Huete, et al., 1997) is designed to enhance the signal of vegetative material by minimizing the effects of background materials, such as soil, litter, and water. The EVI is also designed to have improved sensitivity in high biomass areas. It accomplishes this by de-coupling the canopy background signal and reducing the influence of the atmosphere on the signal. The equation for the EVI is as follows:

$EVI = G*(\rho_{NIR}-\rho_R)/(\rho_{NIR} + C1*\rho_R + C2*\rho_B + L)$

where (adopted values for coefficients in parentheses below)

ρ_{NIR} = NIR Reflectance

ρ_R = Red Reflectance

ρ_B = Blue Reflectance

C1 = Atmosphere Resistance Red correction (6)

C2 = Atmosphere Resistance Blue Correction (7.5)

L = Canopy Brightness Correction Factor (1)

G = Gain Factor (2.5)

This index has a reduced dependence on atmospheric influences because it uses the blue band, which is atmospherically sensitive, to correct the red band (Huete, 1997).

WDRVI

The Wide Dynamic Range Vegetation Index , or WDRVI (Gitelson, 2003), is designed to improve the sensitivity of the NDVI under moderate to high-aboveground biomass conditions, where NDVI saturates. This is accomplished by applying a coefficient to the NIR reflectance signal of the NDVI equation. The equation for the WDRVI is:

$$WDRVI = (\alpha * \rho_{NIR} - \rho_R)/(\alpha * \rho_{NIR} + \rho_R)$$

The basis for applying this coefficient is that, at high biomass conditions, the ratio of NIR/R >>1, so that both the numerator and denominator in the NDVI equation are nearly equal, and changes in the red signal have very little effect on the NDVI signal. The coefficient acts to attenuate the NIR signal, making the equation more sensitive to changes in red reflectance.

VARI

The Visible Atmospherically Resistant Index (VARI) (Gitelson, et al., 2002) is designed as an index for remote estimation of vegetation fraction that uses only the visible portion of the electromagnetic spectrum (~400-700 nm). The VARI equation is:

$VARI = (\rho_G - \rho_R)/(\rho_G + \rho_R - \rho_B)$

By using the concepts developed by the Atmospherically Resistant Vegetation Index (ARVI), which uses reflectance in the blue range of the electromagnetic spectrum to correct for atmospheric effects on the red channel, because the blue channel is highly sensitive to atmospheric effects (Kauffman and Tanre, 1992). This same principle is applied to the VARI, where the blue channel is used to correct the red channel reflectance. The green and red reflectance terms are used because of their sensitivity to changes in vegetation fraction (Gitelson, et al., 2002).

RRDI

The Reciprocal Reflectance Difference Index (RRDI) (Gitelson, 2003) is designed as an estimator of pigment content, specifically chlorophyll. The equation for the RRDI is:

$RRDI = (\rho_G^{-1} - \rho_{NIR}^{-1}) * \rho_{NIR}$ or

$RRDI = (\rho_{RE}^{-1} - \rho_{NIR}^{-1}) * \rho_{NIR}$

It uses reciprocal reflectance at either 550 nm (ρ_G, green on the electromagnetic spectrum) or 700 nm (ρ_{RE}, the red edge on the electromagnetic spectrum), which are related to chlorophyll content in leaves. Either can be used unless there is anthocyanin present in the leaves, then only the 700 nm waveband can be used. The reciprocal NIR reflectance is subtracted from the first term to make the index linearly proportional to

chlorophyll content. The final NIR reflectance term (ρ_{NIR}) attempts to account for scattering by the canopy and for differences in leaf structure.

SAVI

The Soil Adjusted Vegetation Index (SAVI) (Huete, 1988) is based on the NDVI with a term added to adjust for soil brightness influences. The equation for SAVI is:

$SAVI = (\rho_{NIR} - \rho_R)/(\rho_{NIR} + \rho_R + L)*(1+L)$

The L term is introduced in order to minimize the effects of soil brightness. It is a function of canopy density, where, if the canopy completely obscures the soil, L=0, and SAVI = NDVI. The value of L=0.5 was used for this project because this value is recommended for intermediate canopy cover.

GNDVI

The Green Normalized Difference Vegetation Index (GNDVI) (Gitelson, et al., 1996) is also based on the NDVI, but it uses the green portion of the electromagnetic spectrum instead of the red. The equation for the GNDVI is:

$GNDVI = (\rho_{NIR} - \rho_G)/(\rho_{NIR} + \rho_G)$

The goal of this index is to improve the sensitivity of the basic NDVI to chlorophyll. The original index is only sensitive to trace amounts of chlorophyll in leaves. Maximum sensitivity to chlorophyll is found between 520-630 nm and at 700 nm.